NEA/NSC/DOC(97)13
INDC(Ger)-043
Jül-3410

PROGRESS REPORT ON NUCLEAR DATA RESEARCH IN THE FEDERAL REPUBLIC OF GERMANY

for the Period April 1, 1996 to March 31, 1997

July 1997

Edited by
S.M. Qaim
Forschungszentrum Jülich GmbH
Institut für Nuklearchemie
Jülich, Federal Republic of Germany

FOREWORD

As in previous years, this report has been prepared to promote the exchange of nuclear data research information between the Federal Republic of Germany and other member states of OECD/NEA and IAEA. It covers progress reports from the research centres at Karlsruhe and Jülich, the universities of Dresden, Hannover, Köln, Mainz, Marburg, München as well as from the PTB Braunschweig. The emphasis in the work reported here is on measurement, compilation and evaluation of nuclear data for pure and applied science programmes, such as those relevant to fission- and fusion-reactor technology, accelerator shielding and development, astrophysics research, cosmogenic and meteoritic investigations, radiation therapy, production of medically important radioisotopes, etc.

The coordination of nuclear data activities at the international level is done by two committees: the NEA-Nuclear Science Committee (NEA-NSC) and the IAEA-International Nuclear Data Committee (INDC). The present Editor has the privilege and the responsibility of representing Germany in both the committees. This report should therefore serve also as a background information to some areas of work of those committees.

Each contribution is presented under the laboratory heading from where the work is reported. The names of other participating laboratories are also mentioned. When the work is relevant to the World Request List for Nuclear Data, WRENDA 93/94 (INDC(SEC)-104/U+G), the corresponding identification numbers are given.

Jülich, July 1997 S.M. Qaim

CONTENTS

FORSCHUNGSZENTRUM KARLSRUHE
INSTITUT FÜR KERNPHYSIK

Page

1. Measurement of Neutron Capture on ^{48}Ca at Thermal and Thermonuclear Energies
H. Beer, C. Coceva, P.V. Sedyshev, Yu. P. Popov, H. Herndl, R. Hofinger, P. Mohr, H. Oberhummer 1

2. A Moxon-Rae Setup for the Measurement of Stellar (n,γ) Rates and the Example of ^{87}Rb
S. Jaag, F. Käppeler 1

3. Stellar Neutron Capture Cross Sections of the Tin Isotopes
K. Wisshak, F. Voss, Ch. Theis, F. Käppeler, K. Guber, L. Kazakov, N. Kornilov, G. Reffo 2

4. Resonance Neutron Capture in ^{116}Sn, ^{118}Sn, and ^{120}Sn
K. Wisshak, F. Voss, F. Käppeler 2

5. Neutron Capture of the Bottleneck Isotopes ^{138}Ba and ^{208}Pb, s-Process Studies, and the r-Process Abundance Distribution
H. Beer, F. Corvi, P. Mutti 2

ABTEILUNG METALLISCHE WERKSTOFFE
INSTITUT FÜR MATERIALFORSCHUNG I
FORSCHUNGSZENTRUM KARLSRUHE

E. Daum

1. Investigation of Ligh Ion Induced Activation Cross Sections in Iron 4
1.1 Proton induced activation cross sections 4
1.2 Alpha particle induced activation cross sections 6

FORSCHUNGSZENTRUM KARLSRUHE
INSTITUT FÜR NEUTRONENPHYSIK UND REAKTORTECHNIK

1. Validation of the FENDL-1 Nuclear Data Library and Benchmark Testing for FENDL-2 Candidate Evaluations
U. Fischer, E. Wiegner, Y. Wu 9

2. A 14-MeV Neutron Transmission Experiment on Vanadium
U. von Möllendorff, B.V. Devkin, U. Fischer, B.I. Fursov, M.G. Kobozev, M.M. Potapenko, S.P. Simakov, V.A. Talalaev, Y. Wu 11

INSTITUT FÜR NUKLEARCHEMIE
FORSCHUNGSZENTRUM JÜLICH

Page

1. Complex Particle Emission Reactions
M. Faßbender, B. Scholten, S.M. Qaim 13

2. Isomeric Cross Sections
C. Nesaraja, R. Dóczi, F. Cserpák, S. Sudár, J. Csikai, A. Fessler, B. Strohmaier, S.M. Qaim 13

3. Neutron Activation Cross Sections
C. Nesaraja, St. Spellerberg, K.H. Linse, R. Dóczi, F. Cserpák, S. Sudár, J. Csikai, A. Fessler, S.M. Qaim 15

4. Activation Cross Section Data Relevant to Proton Therapy
M. Faßbender, B. Scholten, Yu.N. Shubin, S.M. Qaim 16

5. Excitation Functions Relevant to Radioisotope Production
A. Hohn, P. Reimer, A. Klein, Z. Kovács, F. Tárkányi, S. Takács, A. Fenyvesi, B. Scholten, H.H. Coenen, S.M. Qaim 18

INSTITUT FÜR KERNPHYSIK
FORSCHUNGSZENTRUM JÜLICH

The Production Cross Section and the Lifetime of Heavy Λ Hypernuclei
H. Ohm, W. Borgs, W. Cassing, M. Hartmann, T. Hermes, L. Jarczyk, B. Kamys, H.R. Koch, P. Kulessa, R. Maier, D. Prasuhn, K. Pysz, Z. Rudy, H.J. Stein, A. Strzalkowski, O.W.B. Schult, Y. Uozumi, I. Zychor 22

INSTITUT FÜR KERN- UND TEILCHENPHYSIK
TECHNISCHE UNIVERSITÄT DRESDEN

1. Integral Activation Experiment with 14MeV Neutrons on Steels
H. Freiesleben, V. Kovalchuk, D. Markovskij, D. Richter, K. Seidel, V. Tereshkin, S. Unholzer 23

2. Investigation of Spectral Neutron and Gamma Fluxes in a Fusion Reactor Blanket Mock-up
U. Fischer, H. Freiesleben, W. Hansen, D. Richter, K. Seidel, S. Unholzer, Y. Wu 26

3. Self-Ionization Probabilities after K-Shell Ionization
A. El-Shemi, G. Zschornack 30

4. Measurement of L X-ray Intensity Ratios for Electron Excitation in the Atomic Number Region Z = 47 to 74
D. Küchler, J. Tschischgale, G. Zschornack 33

ABTEILUNG NUKLEARCHEMIE
UNIVERSITÄT ZU KÖLN
AND
ZENTRUM FÜR STRAHLENSCHUTZ UND RADIOÖKOLOGIE
UNIVERSITÄT HANNOVER

Page

1. A New Facility at The Svedberg Laboratory for Parasitic Activation Experiments with Medium-Energy Neutrons
S. Neumann, R. Michel, O. Jonson, P. Malmborg, F. Sudbrock, U. Herpers, B. Holmqvist 35

2. Cross Sections for the Production of Residual Nuclides in Proton-Induced Reactions in Heavy Elements
M. Gloris, R. Michel, U. Herpers, F. Sudbrock, B. Holmqvist, H. Condé, P. Malmborg 37

3. Determination of Cross Sections for the Production of Long-Lived Residual Nuclides ^{10}Be and ^{36}Cl via AMS
F. Sudbrock, A. Berkle, U. Herpers, R. Michel, M. Gloris, B. Holmqvist, H. Condé, P. Malmborg P.W. Kubik, H.-A. Synal, M. Suter 40

INSTITUT FÜR KERNCHEMIE
UNIVERSITÄT MAINZ

1. Proton Odd-Even Effects in the Fission of the Odd-Z Compound Nucleus ^{239}Np (Z=93)
M. Davi, H.O. Denschlag, I. Tsekhanovitch, H.R. Faust, S. Oberstedt, M. Wöstheinrich 43

INSTITUT FÜR KERNCHEMIE
PHILIPPS-UNIVERSTÄT MARBURG

Determination of the Half-Life of ^{105m}Rh
A. Kronenberg, K. Siemon, R. Weber, R.A. Esterlund, P. Patzelt 46

FRM-REAKTORSTATION GARCHING
FACHBEREICH PHYSIK
TECHNISCHE UNIVERSITÄT MÜNCHEN

Interaction of Slow Neutrons with Cobalt and Tin
K. Knopf, W. Waschkowski, A. Aleksejevs, S. Barkanova, J. Tambergs 49

PHYSIKALISCH-TECHNISCHE BUNDESANSTALT BRAUNSCHWEIG Page

1. Measurement of the $^{52}Cr(n,p)^{52}V$ Cross Section between 7.9 and 14.4 MeV
W. Mannhart, D. Schmidt, D.L. Smith 50

2. Measurement of the $^{52}Cr(n,2n)^{51}Cr$ Cross Section between Threshold and 14.4 MeV
W. Mannhart, D. Schmidt, D.L. Smith 51

3. Neutron Scattering on ^{51}V at Energies between 8 MeV and 15 MeV
D. Schmidt, W. Mannhart, Zhou Chenwei 52

4. Double-differential Neutron Emission Cross Sections from Natural Lead in the Energy Region between 8 MeV and 15 MeV
D. Schmidt, W. Mannhart, B.R.L. Siebert 53

5. Half-Life Measurements on Isotopes of Europium
H. Schrader, U. Schötzig 55

APPENDIX

Addresses of Contributing Laboratories 59

FORSCHUNGSZENTRUM KARLSRUHE
INSTITUT FÜR KERNPHYSIK

1. MEASUREMENT OF NEUTRON CAPTURE ON ^{48}Ca AT THERMAL AND THERMONUCLEAR ENERGIES

H. Beer, C. Coceva[1], P. V. Sedyshev[2], Yu. P. Popov[2], H. Herndl[3], R. Hofinger[3], P. Mohr[3], and H. Oberhummer[3]

At the Karlsruhe pulsed 3.75 MV VdG accelerator the thermonuclear ^{48}Ca(n,γ)^{49}Ca cross section was measured by the fast cyclic activation technique via the 3084.4 keV γ-ray line of the ^{49}Ca-decay. Samples of $CaCO_3$ enriched in ^{48}Ca to 77.87 % were irradiated between two gold foils which served as capture standards. The capture cross-section was measured at the neutron energies 25, 151, 176, and 218 keV, respectively. Additionally, the thermal capture cross-section was measured at the reactor BR1 in Mol, Belgium, via the prompt and decay γ-ray lines using the same target material. The ^{48}Ca(n,γ)^{49}Ca cross-section in the thermonuclear and thermal energy range has been calculated using the direct-capture model combined with folding potentials. The potential strengths are adjusted to the scattering length and the binding energies of the final states in ^{49}Ca. The small coherent elastic cross section of ^{48}Ca+n is explained through the nuclear Ramsauer effect. Spectroscopic factors of ^{49}Ca have been extracted from the thermal capture cross-section with better accuracy than from a recent (d,p) experiment. Within the uncertainties both results are in agreement. The non-resonant thermal and thermonuclear experimental data for this reaction can be reproduced using the direct-capture model. A possible interference with a resonant contribution is discussed. The neutron spectroscopic factors of ^{49}Ca determined from shell-model calculations are compared with the values extracted from the experimental cross sections for ^{48}Ca(d,p)^{49}Ca and ^{48}Ca(n,γ)^{49}Ca.

Phys. Rev. C* **54 (1996) 2014

2. A MOXON-RAE SETUP FOR THE MEASUREMENT OF STELLAR (n,γ) RATES AND THE EXAMPLE OF ^{87}Rb*

S. Jaag and F. Käppeler

A setup with Moxon-Rae detectors was optimized for measurements of (n,γ) cross sections in the keV–region. The technique is particularly suited for the determination of

[1]E.N.E.A, Bologna, Italy
[2]Frank Laboratory of Neutron Physics, JINR, Dubna, Russia
[3]Institut für Kernphysik, TU Wien, Vienna, Austria

Maxwellian–averaged cross sections for nucleosynthesis studies related to s–process scenarios. The experimental technique makes use of the quasi–Maxwellian spectrum that can be obtained via the ^{7}Li (p,n) ^{7}Be reaction. It allows measurements at extremely short flight paths with the time–of–flight method as an option for background reduction. The experimental determination of the efficiency with calibrated γ–sources and with two–step cascades from selected resonances of the ^{34}S(p,γ) reaction revealed new properties of the response function. The reliability of the new method was first demonstrated via the example of the well known ratio of the (n,γ) cross sections of Ta and Au, and then used for a measurement of the stellar ^{87}Rb cross section. With this new value, $< \sigma v > /v_T = 15.5 \pm 1.5$ mb, a discrepancy in the previously existing data could be resolved.

Phys. Rev. C* **53 (1996) 2474

3. STELLAR NEUTRON CAPTURE CROSS SECTIONS OF THE TIN ISOTOPES*

K. Wisshak, F.Voss, Ch.Theis, F. Käppeler, K. Guber[1], L. Kazakov[2], N. Kornilov[2], G. Reffo[3]

The neutron capture cross sections of ^{114}Sn, ^{115}Sn, ^{116}Sn, ^{117}Sn, ^{118}Sn, and ^{120}Sn were measured in the energy range from 3 to 225 keV at the Karlsruhe 3.75 MV Van de Graaff accelerator. Neutrons were produced via the ^{7}Li(p,n)^{7}Be reaction using a pulsed proton beam. Capture events were registered with the Karlsruhe 4π Barium Fluoride Detector. The experiment was difficult due to the small (n,γ) cross sections of the proton magic tin isotopes, and due to the comparably low enrichment of the rare isotopes ^{114}Sn and ^{115}Sn. This caused significant corrections for capture of scattered neutrons and for isotopic impurities, but the high efficiency and the spectroscopic quality of the BaF_2 detector allowed to determine these corrections reliably. Typical overall uncertainties of 1–2% could be achieved for the cross section ratios, five times smaller compared to existing data. Based on these results, Maxwellian averaged (n,γ) cross sections were calculated for thermal energies between kT = 10 keV and 100 keV.

Phys. Rev. C* **54 (1996) 1451

4. RESONANCE NEUTRON CAPTURE IN ^{116}Sn, ^{118}Sn, AND ^{120}Sn*

K. Wisshak, F.Voss, F. Käppeler

The neutron capture cross sections of ^{116}Sn, ^{118}Sn, and ^{120}Sn, which were determined recently with the Karlsruhe 4π barium fluoride detector, has been reanalyzed in the low energy region using a shape analysis program. Resonance parameters were extracted

[1]Oak Ridge National Laboratory, Oak Ridge, USA
[2]Institute for Physics and Power Engineering, Obninsk, Russia
[3]ENEA, Centro Dati Nucleari, Bologna, Italy

which allow a more reliable determination of the averaged cross section below 20 keV. The results confirm our first analysis and the reported stellar cross sections. Accordingly, the results of the s–process studies based on these data remain unchanged.

Phys. Rev. C* **54 (1996) 2732

5. NEUTRON CAPTURE OF THE BOTTLENECK ISOTOPES ^{138}Ba AND ^{208}Pb, s-PROCESS STUDIES, AND THE r-PROCESS ABUNDANCE DISTRIBUTION*

H. Beer, F. Corvi[1], and P. Mutti[1]

The capture cross sections of ^{138}Ba and ^{208}Pb have been measured by time–of–flight (TOF) at the electron linear accelerator GELINA in the energy range 200 eV to 200 keV. The Maxwellian averaged capture (MAC) cross sections were determined *vs* temperature kT between 5 and 100 keV. The data were applied to carry out new parametric studies of the s–process. Two parametrized models were considered, pulsed s–process with one neutron source and double pulsed s–process, the combined burning of two neutron sources. Through the s–process abundance distribution the complementary semiempirical p–process and r–process abundance distributions were determined. Especially the termination of the s-process was investigated. It was found that in the frame of the double pulse s–process model only negligible amounts of ^{209}Bi are synthesized. This would mean that bismuth is mainly an r–process element.

Astrophys. J.* **474 (1997) 843

[1]CEC, JRC, IRMM, Geel, Belgium

ABTEILUNG FÜR METALLISCHE WERKSTOFFE
INSITUT FÜR MATERIALFORSCHUNG I
FORSCHUNGSZENTRUM KARLSRUHE

E. Daum

1 Investigation of light ion induced activation cross sections in iron

In the framework of the development of low activation iron based steels for fusion reactor applications, e.g. first wall materials, experimental and theoretical investigations regarding activation with high energy light ions as protons and alpha particles have been done. Light ions are used in this field in simulation irradiation experiments.
The main focus of this work was put on pure iron which constitutes with about 90 % to the low activation iron based steels. The experiments were done at the cyclotrons of the Forschungszentrum Karlsruhe.
In the experiments thin rolled high purity iron foils (thickness < 20 µm) were irradiated. The protons used had a primary energy of 30 MeV which could be moderated by carbon or steel degraders to 10 MeV. The alpha particles used had a primary energy in the range of 35 MeV (internal beam with variable energy) through 104 MeV (external beam with fixed energy) which could be moderated by steel degraders. The induced activation was measured by gamma spectroscopy with a LN_2-cooled high purity Ge detector. The data measurement and evaluation was automated by PC. It should be noted that a lot of effort was put on the detection of the short half-life nuclides with $T_{1/2}$ of a few minutes ($^{53}Fe_g$, $^{53}Fe_m$, $^{52}Mn_m$ and ^{52}V) which could be measured for the first time.
The measured excitation functions were complemented by theoretical calculations with the ALICE code [1] which uses the geometry dependent hybrid model for the precompound nuclear reactions and the Weißkopf-Ewing evaporation model for the compound nuclear reactions. Additionally, different nuclear level densities, the Fermi level density (FLD) and the Kataria-Ramamurthy level density (KRLD), were used. The excitation functions were calculated for protons and alpha particles from reaction threshold energy up to primary energy in 1 MeV steps. All open reaction channels were considered. The results were compared to literature data if available. These investigation lead to a comprehensive set of light ion activation data for iron.

1.1 Proton induced activation cross sections

The nuclides produced in ^{nat}Fe under proton irradiation are listed in table 1. The data are plotted in figure 1. For the most reaction channels a lot of experimental data were found in the literature except for ^{54}Mn. For this nuclide the data could be extended in the energy range from 10 through 30 MeV. The comparison with theoretical data shows qualitatively a good agreement. The reaction threshold energies - a discussion is in most cases only possible for the lowest energy - are also reasonable. The quantitative comparison shows a good agreement in single cases; however, differences up to one order of magnitude can appear. For the nuclide ^{55}Co previous ALICE calculations from 1982 are found. This shows the nuclear model development during the years 1982 to 1991.

Table 1: Collection of all proton induced nuclides in iron

Type of reaction	Produced nuclides
(p, xn)	$^{58}Co_g$, ^{57}Co, ^{56}Co, ^{55}Co
(p, pxn)	$^{53}Fe_g$
(p, 2pxn) and (p, αxn)	^{54}Mn, $^{52}Mn_g$

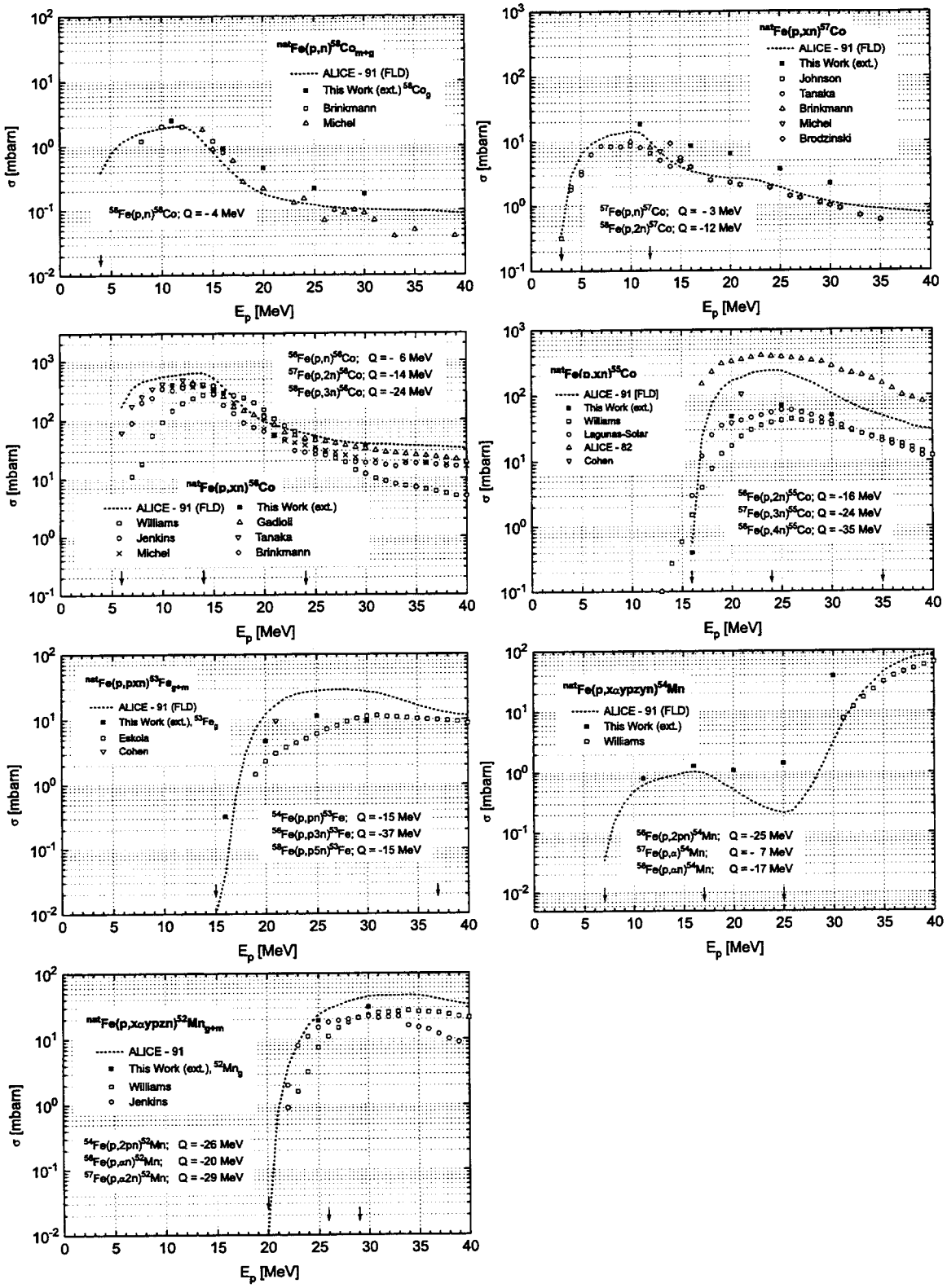

Figure 1: Proton induced excitation functions in ^{nat}Fe. The solid squares show the data measured in this work (ext. = external beam). The open symbols show literature data. The corresponding citations can be found in [2]. The dotted line gives a comparison to nuclear model calculations with ALICE. The arrows point to the Q values of the reaction channels which are listed in the plots.

1.2 Alpha particle induced activation cross sections

The nuclides produced in ^{nat}Fe under alpha particle irradiation are listed in table 2. The data are plotted in figure 2. For the long-lived nuclides plenty of experimental data were found in the literature. For the short-lived nuclides the measurements and theoretical calculations are provided for the first time. For the model calculations two different nuclear level densities have been used. In general it can be stated that in the Ni and Co domain KRLD fits better than FLD. In the other cases it is not obvious which model of both is the best. It depends on the cases, varies also with energy and can differ up to one order of magnitude. As with the proton data, the reaction threshold energies are reasonable. The quantitative comparison shows the best agreement in the Co domain and a good agreement in further single cases. In general the theoretical data differ more if the residualnuclide gets lighter. As worst cases can be pointed out the ^{52}V and ^{47}Sc where the nuclear model is far away from the experiment.

Table 2: Collection of all alpha particle induced nuclides in iron

Type of reaction	Produced nuclides
(α,xn)	^{57}Ni, ^{56}Ni
(α,pxn)	$^{58}Co_g$, ^{57}Co, ^{56}Co, ^{55}Co
(α,αxn)	$^{53}Fe_{g+m}$, $^{52}Fe_g$
(α,3pxn) and (α,αpxn)	^{56}Mn, ^{54}Mn, $^{52}Mn_{g+m}$
(α,α2pxn) and (α,2αxn)	^{51}Cr, ^{49}Cr
(α,5pxn),(α,α3pxn) and (α,2αpxn)	^{52}V, ^{48}V
(α,2α3p) and (α,3αpxn)	^{47}Sc

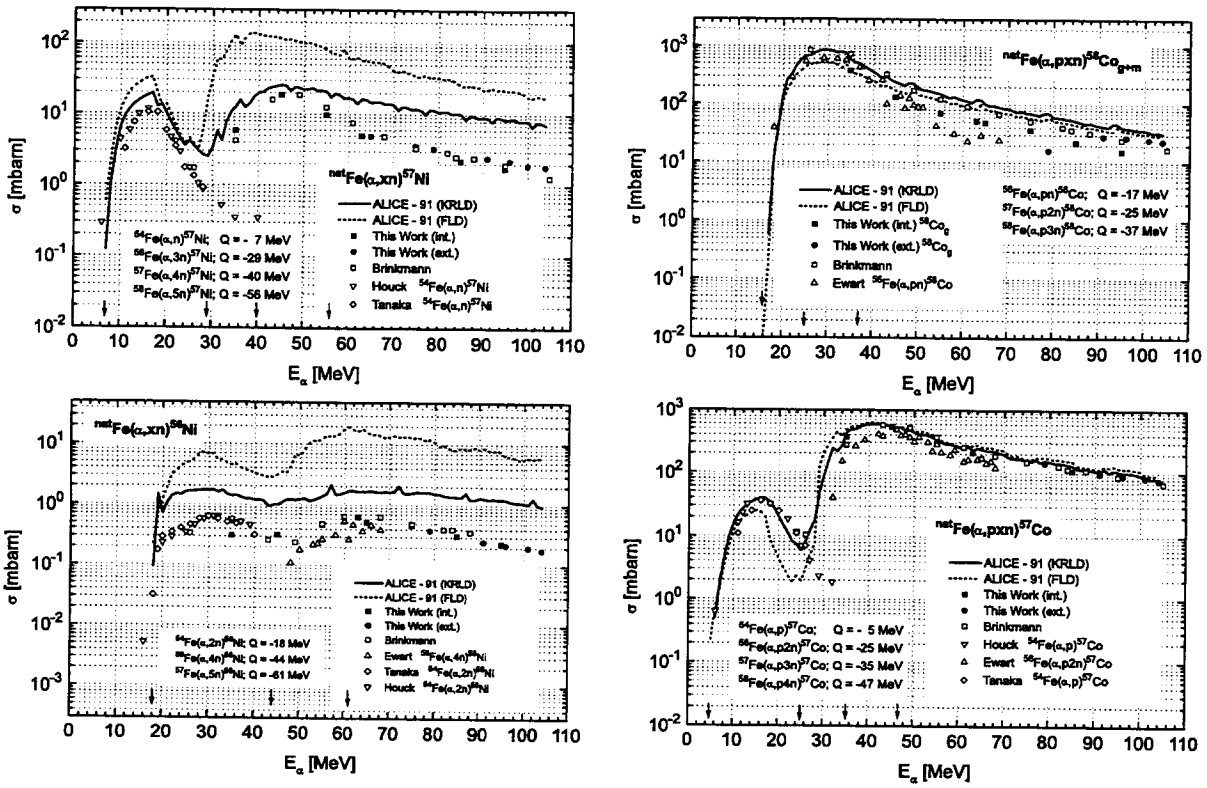

Figure 2 continued (for caption see page 8)

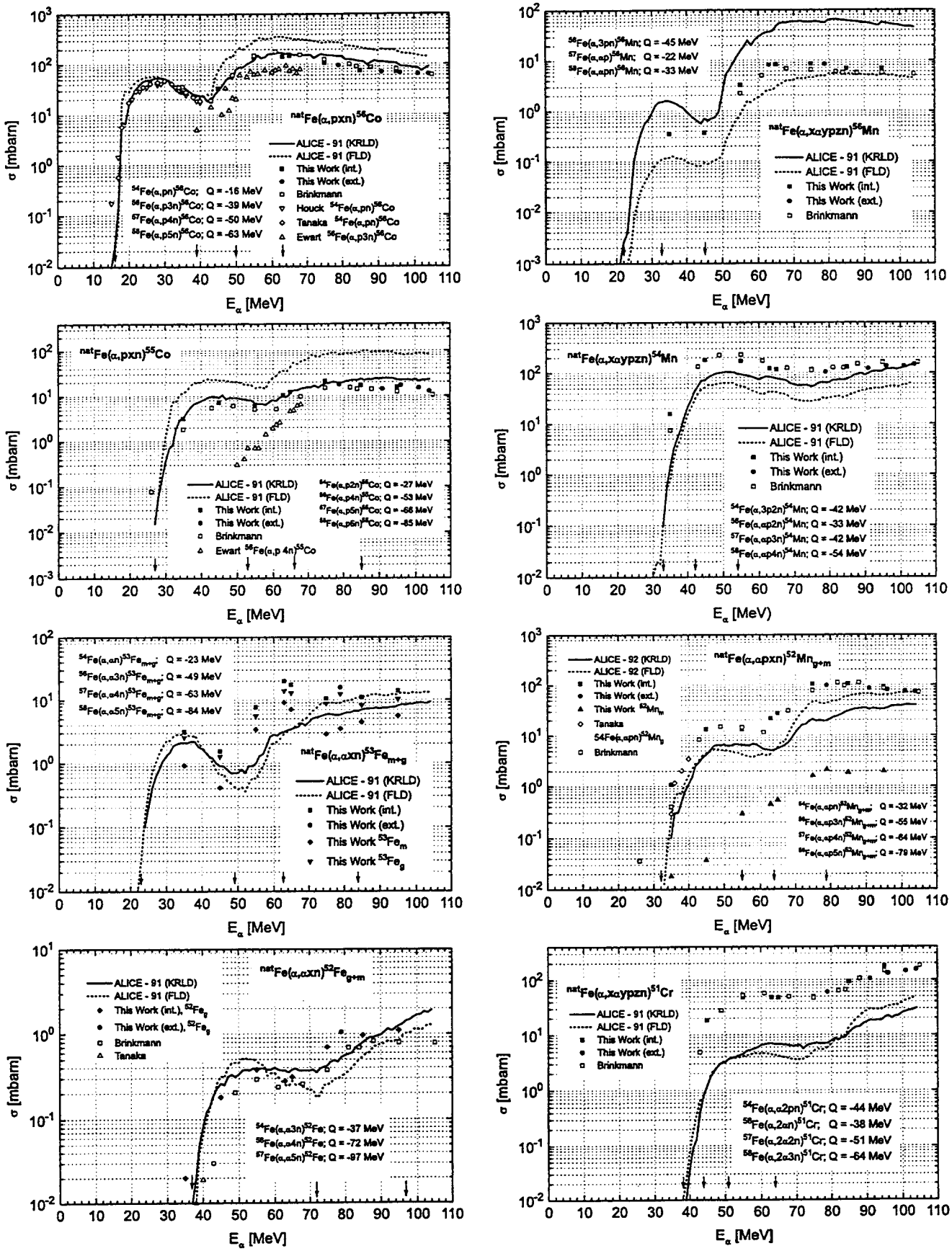

igure 2 continued (for caption see page 8)

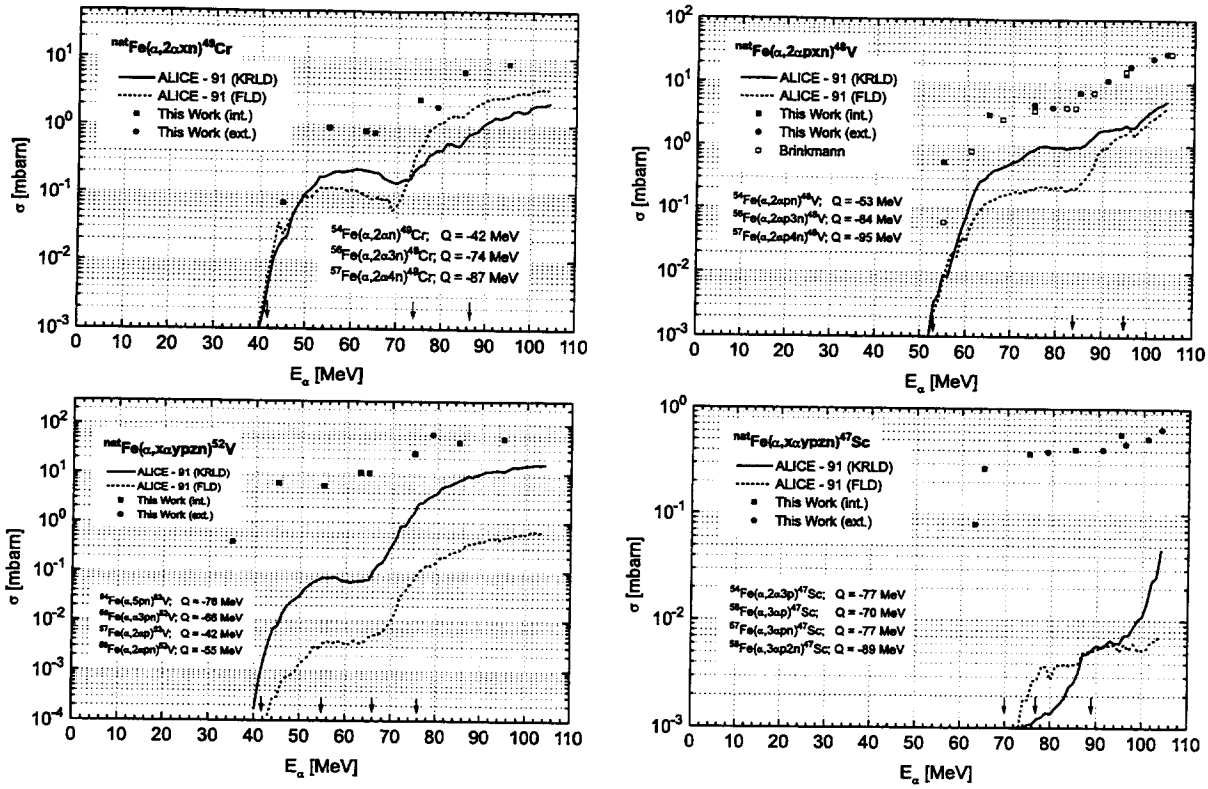

Figure 2: Alpha particle induced excitation functions in ^{nat}Fe. The solid squares and circles show the data measured in this work (ext. = external / int. = internal beam). The open symbols show literature data. The corresponding citations can be found in [2]. The solid (KRLD) and dotted (FLD) lines give a comparison to nuclear model calculations with ALICE. The arrows point to the Q values of the reaction channels which are listed in the plots.

References

1. M. Blann, CODE ALICE/85/300, UCID-20169, Lawrence Livermore National Lab., Sept. 1994
2. E. Daum, *Theoretische und experimentelle Untersuchungen zur Schädigung und Aktivierung von reinem Eisen unter Bestrahlung mit höherenergetischen leichten Ionen*, FZKA 5833, Forschungszentrum Karlsruhe, Oktober 1996

FORSCHUNGSZENTRUM KARLSRUHE
INSTITUT FÜR NEUTRONENPHYSIK UND REAKTORTECHNIK

1. Validation of the FENDL-1 Nuclear Data Library and Benchmark Testing for FENDL-2 Candidate Evaluations

U. Fischer, E. Wiegner, Y. Wu

The Fusion Evaluated Nuclear Data Library (FENDL) is a compilation of fusion-oriented data files selected from the nuclear data libraries ENDF/B-VI (USA), BROND (Russian Federation), JENDL (Japan) and EFF (European Fusion File) in an international effort initiated and co-ordinated by the IAEA Nuclear Data Section [1]. The first version of the data file FENDL-1 has been released in 1994 and was recommended as reference library for design calculations in the Engineering and Designn Activity (EDA) phase of the International Thermonuclear Experimental Reactor (ITER) project.

An international benchmark validation task, co-ordinated by Forschungszentrum Karlsruhe (FZK), has been conducted recently to validate FENDL-1 through data tests against integral 14-MeV neutron experiments [2, 3]. The main objective of this task was to qualify the FENDL-1 working libraries for fusion applications and to elaborate recommendations for further data improvements. A large variety of existing integral 14 MeV benchmark experiments has been analysed with the FENDL-1 working libraries for continuous energy Monte Carlo (FENDL/MC-1.0) and multigroup discrete ordinates (FENDL/MC-1.0) calculations by laboratories and institutions from the European Union, Japan, the Russion Federation and the United States. The major findings of the benchmark analyses are given for three categories of fusion reactor materials in Tables Ia - Ic below. With regard to data quality, it was summarised that fusion nuclear data have reached a high confidence level with the available FENDL-1 data library. With few exceptions this is true for the materials of highest importance for fusion reactor applications. As a result of the performed benchmark analyses, some still existing deficiencies and discrepancies have been identified and recommendations were given for further improvements to be included in the forthcoming FENDL-2 data file.

Based on these recommendations, a priority list was adopted of FENDL-2 candidate evaluations considered for replacement of current FENDL-1 evaluations [4]. The materials included were Be, V, Fe, W (first priority), C, O, Al, Si, Zr (second priority) and D, N, Nb, Mo, Sn (third priority). As part of the selection procedure, the candidate evaluations from the data files JENDL-FF (Japan), ENDF/B-VI (USA), BROND (RF) and EFF-2, -3 were benchmarked against available integral experiments and FENDL-1 test calculations. The benchmark analyses were performed by means of coupled neutron-photon transport calculations with the Monte Carlo code MCNP4A, the discrete ordinates code ONEDANT and the nodal transport code NGSN/1D. The analysed experiments cover a wide range of fusion-relevant materials. In particular, 14 MeV neutron transmission experiments on rectangular iron and beryllium slabs, and on spherical iron, beryllium, aluminium, silicon and molybdenum shells with measurements of neutron leakage spectra were analysed.

In general, the analysed new EFF and JENDL-FF data evaluations show better agreement with integral experiments than do the existing FENDL-1 data. In particular this is true for iron, aluminium, silicon and zirconium. Some remarkable exceptions to this rule were caused by deficiencies in the current working libraries that have been revised meanwhile.

Based on the data testing results and a careful review of the submitted cross-section evaluations, the selection shown in Table 2 was adopted for the new FENDL-2 evaluations [5, 6].

Table Ia - Ic: Major findings of the FENDL-1 integral data tests [2, 3].

Table Ia: Neutron multiplication and breeding materials

Element	Data quality	Comments
Be	improvements needed	SED/SAD[1] to be improved; discrepant integral experiments need to be clarified
Pb	satisfactory	
Li	satisfactory	
Al, Si, Zr	improvements needed	SED to be improved; γ - production to be improved for Si

Table Ib: Structural and/or shielding materials

Element	Data quality	Comments
Fe	improvements needed	fluctuation factors to be included in partial neutron cross-sections; need for including anisotropic γ-emission data indicated
Cr	improvements needed	need for additional integral experiments; γ-production to be improved
Cu	improvements needed	SED in 5-10 MeV range and below 1 MeV to be improved
Mn	satisfactory	need for additional integral experiments
Ni	unclear	urgent need for new integral experiment
W	improvements needed	improvements for SED and γ-production needed
SS-316	improvements needed	disagreement for high and intermediate energy range of neutron spectrum
V	unclear	need for more integral experiments

Table Ic: Other materials

Element	Data quality	Comments
C	improvements needed	SED needs improvement
N	improvements needed	SED/SAD needs improvement
O	improvements needed	SED/SAD needs improvement
F	improvements needed	large discrepancies observed in integral data tests; SED possibly to be improved
Ti	improvements needed	SED needs improvement
Co	improvements needed	SED needs improvement; need for more integral experiments
Nb	improvements needed	SED needs improvement; γ-production to be improved
Mo	satisfactory	minor discrepancy in neutron spectrum

Table 2: New evaluations for the FENDL-2 [5, 6]

JENDL-FF	^{9}Be, ^{12}C, ^{14}N, ^{16}O, ^{51}V, ^{nat}Zr, ^{93}Nb, ^{nat}Mo, ^{nat}W
EFF-3	^{27}Al, ^{56}Fe
ENDF/B-VI	$^{28, 29, 30}Si$
BROND-2	^{2}H, ^{nat}Sn

[1] SAD/SED means secondary energy/angle distribution

References

[1] D.W. Muir, S. Ganesan and A.B. Pashchenko: "FENDL - A reference nuclear data library for fusion applications", Int. Conference on Nuclear Data for Science and Technology, May 13 - 17, 1991, Juelich, Germany.

[2] U. Fischer et al., Benchmark Validation of the FENDL-1 Nuclear Data Library - A Co-ordinated International Effort, Fusion Technology Vol. 30, No. 3, Part 2B (Dec. 1996), 1093 - 1100.

[3] U. Fischer (Ed.), Integral Data Tests of the FENDL-1 Nuclear Data Library for Fusion Applications, FZKA-5785, INDC(GER)-41, August 1996.

[4] A.B. Pashchenko, Summary Report of the IAEA Advisory Group Meeting on Completion of FENDL-1 and Start of FENDL-2, Del Mar, CA, December 5-9, 1995, INDC(NDS)-352, March 1996.

[5] A.B. Pashchenko, Summary Report of the IAEA Consutants' Meeting on Selection of Basic Evaluations for the FENDL-2 Library, Karlsruhe, June 24-28, 1996.

[6] IAEA Advisory Group Meeting on Extension and Improvement of the FENDL Library for Fusion Applications (FENDL-2), Vienna, March 3-7, 1997.

2. A 14-MeV neutron transmission experiment on vanadium

U. von Möllendorff[a], B.V. Devkin[b], U. Fischer[a], B.I. Fursov[b], M.G. Kobozev[b], M.M. Potapenko[c], S.P. Simakov[b], V.A.Talalaev[b] and Y. Wu[a,+]

Vanadium-based alloys have, for several reasons, a high potential as structural materials of fusion power reactors. For a reliable assessment of the neutron economy of vanadium, i.e., the balance between (n,2n) multiplication on one hand and absorption reactions on the other, its evaluated nuclear data should be verified, „benchmarked", by integral experiments, i.e., experiments on thick samples. The well-known spherical-shell transmission method with spectrometry of the leakage flux is particularly suited because its simple geometry facilitates both measurements and calculations. The experiment reported here appears to be the first integral fast-neutron experiment ever performed on vanadium.

The work was performed at the KG-0.3 neutron generator in Obninsk. The experimental technique closely followed earlier descriptions [1, 2]. The time-of-flight spectrometer with 6.8 m flight path uses a p-terphenyl scintillator crystal, which has a higher light output than the more usual liquid scintillators. Data can thus be obtained down to neutron energies as low as 50-100 keV. Two massive vanadium spheres (purity >99%) having outer radii of 5 cm and 12 cm were used. For accommodating the neutron source, i.e. the target assembly of the neutron generator, either sphere has a radial hole of radius 1.5 cm, the bottom of which is hemispheric and concentric with the sphere surface.

Three-dimensional Monte-Carlo calculations were made with the MCNP-4A code [3] and evaluated nuclear data for either natural vanadium or V-51 (which is 99.75% of natural V) from the EFF-3, FENDL-1 and JENDL-FF libraries.

The results are shown in the table. The measured quantity Φ is the normalized spectral leakage fluence, or number of leakage neutrons per source neutron, integrated over a leakage energy window as indicated (partial leakage multiplication). The sum of this column is the total leakage multiplication, neglecting the fraction of neutrons below 0.1 MeV. The total uncertainty of Φ, including correlated components such as the source monitoring uncertainty, is estimated at ±7%. All calculations overestimate the total leakage multiplication, JENDL-FF giving the highest results. The partial multiplication results show considerable variations with energy, both above and below unity, which partly compensate each other in the sums. Similar compensation effects were observed earlier in case of calculated leakage multiplications in beryllium. They show that the spectral, and not only the total, leakage neutron fluence should be measured to make this type of experiment useful as a nuclear data benchmark. The overestimations below 0.4 MeV by FENDL-1 and JENDL-FF are considerable.

Although the overestimation is, for most of the results, not larger than the experimental uncertainty, we cautiously conclude that the effective neutron multiplication in vanadium is slightly lower than calculated by present-day nuclear data.

More details are reported in Ref.[4].

[a] Forschungszentrum Karlsruhe GmbH, Institut für Neutronenphysik und Reaktortechnik, Postfach 3640, 76021 Karlsruhe, Germany

[b] State Scientific Center of the Russian Federation, Institute of Physics and Power Engineering, 1 Bondarenko Sq., 249020 Obninsk, Russia

[c] State Scientific Center of the Russian Federation, Science and Research Institute of Inorganic Materials, 5 Rogov st., 123060 Moscow, Russia

[+] Permanent address: Institute of Plasma Physics, Academia Sinica, Hefei, Anhui, P.R. China

Measured normalized neutron leakage fluences Φ (see text) and calculation-over-experiment ratios C/E

	Energy range MeV	Φ	C/E EFF-3	C/E FENDL-1	C/E JENDL-FF
Sphere 1	0.1 - 0.2	0.0128	1.05	1.56	1.37
	0.2 - 0.4	0.0278	0.95	1.25	1.35
	0.4 - 0.8	0.0549	1.01	1.04	1.28
	0.8 - 1.4	0.0712	1.05	0.92	1.04
	1.4 - 2.5	0.0694	1.18	1.00	1.07
	2.5 - 4.0	0.0415	1.14	1.13	1.01
	4.0 - 6.5	0.0274	1.02	1.19	1.10
	6.5 - 10.5	0.0200	0.77	0.88	1.11
	10.5 - 20.0	0.7351	1.00	1.00	0.99
	total	1.060	1.016	1.016	1.035
Sphere 2	0.1 - 0.2	0.0508	1.36	1.71	1.77
	0.2 - 0.4	0.0959	0.94	1.08	1.25
	0.4 - 0.8	0.1725	0.95	0.93	1.13
	0.8 - 1.4	0.1726	1.04	0.92	1.00
	1.4 - 2.5	0.1208	1.19	1.04	1.03
	2.5 - 4.0	0.0599	1.15	1.14	0.98
	4.0 - 6.5	0.0357	1.07	1.22	1.17
	6.5 - 10.5	0.0235	0.87	0.97	1.28
	10.5 - 20.0	0.3792	1.01	1.00	0.97
	total	1.111	1.039	1.037	1.082

ACKNOWLEDGEMENTS

This work has been supported by grant no. 414-GUS-1095H of the German Federal Ministry for Research and Technology. Part of the work was also supported by International Atomic Energy Agency research contract 9268/RB.

REFERENCES

1.S.P. Simakov, A.A. Androsenko, P.A. Androsenko et al., in: Fusion Technology 1992 (C. Ferro et al., eds.), Elsevier, Amsterdam, 1993, p. 1489

2.B.V. Devkin, V.G. Demenkov, M.G. Kobozev et al., Leakage Neutron Spectra from Al, Ni and Ti Spheres with a 14 MeV Neutron Source, report INDC(CCP)-378, Int. Atomic Energy Agency, Vienna, 1994

3.J.F. Briesmeister (ed.), report LA-12625-M, 1993

4.U. von Möllendorff et al., Proc.19th Symposium on Fusion Technology, Lisbon, Sept. 16-20, 1996 (to appear)

INSTITUT FÜR NUKLEARCHEMIE
FORSCHUNGSZENTRUM JÜLICH

1. Complex Particle Emission Reactions

M. Faßbender, B. Scholten, S.M. Qaim

In continuation of our fundamental studies on complex particle emission reactions [cf. 1] we performed radiochemical investigations on the (p,^{7}Be) process on Si, P, S and Cl over the proton energy range of 100 to 200 MeV, and the systematics of the (p,^{7}Be) excitation functions were completed. A few correlations were observed; all of them support the observation that the (p,^{7}Be) cross section decreases as a function of mass and charge of the target nucleus.

2. Isomeric Cross Sections

C. Nesaraja, R. Dóczi*, F. Cserpák*, S. Sudar*, J. Csikai*, A. Fessler†, B. Strohmaier††, S.M. Qaim

Extending our on-going studies on isomer distribution in nuclear reactions [cf. 2], emphasis was now placed on three new investigations:

(a) The formation of the isomeric pair ^{69m,g}Zn in ^{70}Zn(n,2n)-, ^{69}Ga(n,p)- and ^{72}Ge(n,α)-processes in the energy range of 6 to 12 MeV is under study. The aim is to investigate the effect of reaction channels on the isomer distribution.

(b) Comparative studies on the ^{107}Ag(n,p)^{107m,g}Pd and ^{109}Ag(n,p)^{109m,g}Pd processes in the energy range of 6 to 15 MeV are being performed. Since both the target nuclei have the same spin ($1/2^-$) and the residual isotopes from the (n,p) reactions, viz. ^{107m,g}Pd and ^{109m,g}Pd, have similar spins ($I_g = 5/2^+$; $I_m = 11/2^-$), it was postulated that the excitation functions of (n,p) reactions on both ^{107}Ag and ^{109}Ag would have the same shape. The measured results on the ^{107}Ag(n,p)^{107m}Pd and ^{109}Ag(n,p)^{109m}Pd processes are given in Fig. 1 (A) and (B), respectively.

---

* Institute of Experimental Physics, Kossuth University, Debrecen, Hungary
† Mainly at IRMM, Geel, Belgium
†† Institut für Radiumforschung und Kernphysik, Universität Wien

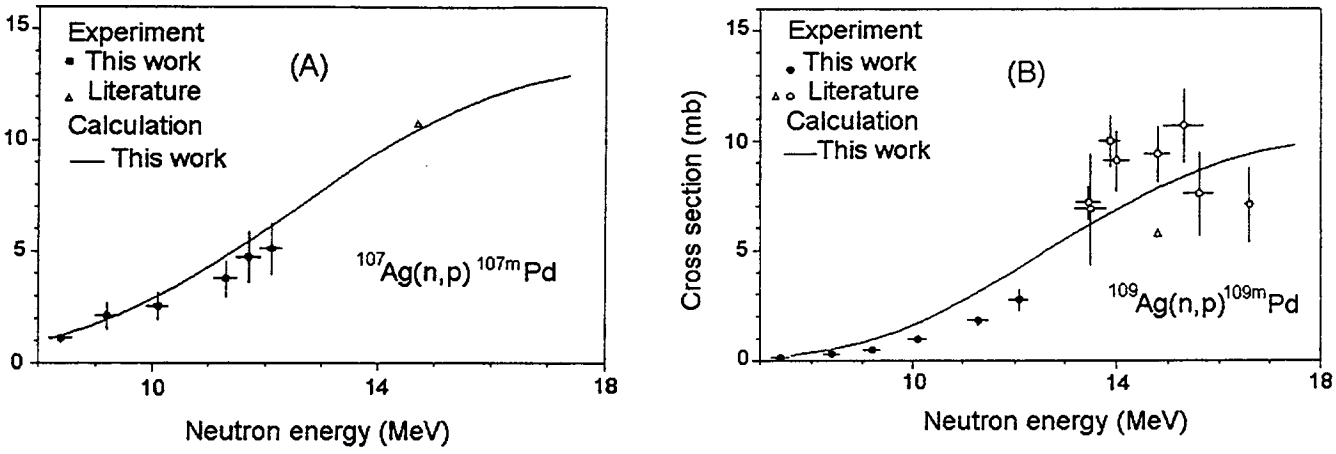

Fig. 1 Comparison of excitation functions for the activation of metastable states ^{107m}Pd(I = 11/2$^-$) and ^{109m}Pd (I = 11/2$^-$) in (n,p) reactions on ^{107}Ag and ^{109}Ag, respectively.

Nuclear model calculations were done using the code STAPRE. The theory reproduces the two excitation functions well, although in both the cases isomeric states are involved. The shapes of the two curves are the same. It is, therefore, concluded that when the spins of the respective targets and products are identical, the excitation curves are also identical. (for more details [cf. 3])

(c) The formation of high-spin isomers ^{195m}Hg and ^{197m}Hg in ^{194}Pt(^{3}He,2n)- and ^{196}Pt(^{3}He,2n)- processes, respectively, in the energy range of 10 to 36 MeV is the subject of the third investigation. First results obtained appear to be very interesting. Somewhat similar studies have been performed on the products ^{52m,g}Fe and ^{53m,g}Fe, which also have rather high-spin isomers.

In addition to the above mentioned three extensive and systematic studies, several other individual isomeric cross sections were measured as a function of energy, e.g. for the ^{89}Y(n,n')^{89m}Y and ^{89}Y(n,α)^{86m}Rb processes. Furthermore, the formation of ^{94m,g}Tc was considered in detail. Nuclear model calculations were done at Vienna for ^{94}Mo(p,n)-, ^{92}Mo(α,pn)- and ^{93}Nb(^{3}He,2n)- processes and the results found to be consistent. (for details [cf. 4]).

3. Neutron Activation Cross Sections

C. Nesaraja, St. Spellerberg, K.H. Linse, R. Dóczi*, F. Cserpák*, S. Sudár*, J. Csikai*, A. Fessler†, S.M. Qaim

(Relevant to request identification numbers: 92 10 04 F, 92 10 09 M, 92 10 56 R, 92 10 57 R, 92 10 69 R, 92 31 40 R, 92 30 28 F)

After completion of the work [cf. 5-7] on the formation of some long-lived activation products like ^{63}Ni ($T_{½}$ = 100 a), ^{88}Y ($T_{½}$ = 106.6 d), ^{89}Sr ($T_{½}$ = 50.6 d), ^{108m}Ag ($T_{½}$ = 433 a), ^{150m}Eu ($T_{½}$ = 36.9 a) and ^{158}Tb ($T_{½}$ = 180 a), partly under the auspices of a CRP of the IAEA, attention was now diverted to the study of some short-lived activation products. Excitation functions of the following reactions are being measured in the neutron energy range of 6 to 12 MeV: $^{52}Cr(n,p)^{52}V$, $^{53}Cr(n,p)^{53}V$, $^{67}Zn(n,p)^{67}Cu$, $^{68}Zn(n,\alpha)^{65}Ni$, $^{69}Ga(n,p)^{69g}Zn$, $^{70}Ge(n,p)^{70}Ga$, $^{107}Ag(n,\alpha)^{104m}Rh$ and $^{109}Ag(n,\alpha)^{106}Rh$. The $^{58}Ni(n,\alpha)^{55}Fe$ and $^{50}Cr(n,n'p)^{49}V$ reactions are under investigation in the neutron energy range of 14 to 20 MeV in collaboration with the IRMM Geel. In studies on the β^- emitting radioisotopes ^{69g}Zn and ^{70}Ga as well as on the soft x-ray emitters ^{49}V and ^{55}Fe, elaborate chemical separations were performed and thin sources prepared. Nuclear model calculations using the code STAPRE are underway to study the reaction mechanisms. In general, the statistical model incorporating precompound effects can describe the emission of protons and α-particles fairly well, provided the input parameters are properly chosen.

In addition to excitation function measurements, some integral tests of differential data were also performed. Using a 14 MeV d(Be) neutron source integral cross sections were measured for the reactions $^{89}Y(n,2n)^{88}Y$, $^{89}Y(n,p)^{89}Sr$ and $^{89}Y(n,\alpha)^{86}Rb$. The data were compared with the integrated data obtained from the known excitation function and the neutron spectral distribution. In general, the agreement was found to be within an error of ± 10%.

---

* Institute of Experimental Physics, Kossuth University, Debrecen, Hungary

† Mainly at IRMM, Geel, Belgium

4. Activation Cross Section Data Relevant to Proton Therapy

M. Faßbender, B. Scholten, Yu.N. Shubin*, S.M. Qaim

Part of the work in this direction was completed. The results on the (p,^{7}Be) reaction have been mentioned above. Studies on the formation of ^{22}Na and ^{24}Na in the interactions of protons of energies between 60 and 250 MeV with Al, Si, P, S, Cl, Ca, Cu and Zn yielded new data. For comparison, the precompound hybrid code ALICE-IPPE was used to calculate the excitation functions. As an example, the excitation function of the ^{nat}Cl(p,x)^{22}Na process is given in Fig. 2. The agreement between experiment and theory is good up to about 140 MeV; at higher energies there is a large deviation. [cf. 8].

Excitation functions of (p,x) processes on Cu, Zn and brass leading to the formation of ^{67}Ga, ^{62}Zn, ^{55,56,57,58}Co, ^{52,54}Mn, ^{48}V and ^{51}Cr were determined [9]. A good agreement was found between experiment and theory for products in the vicinity of the target nucleus; large deviations were, however, observed for energies above 120 MeV and for product nuclei rather away from the target nucleus.

* Institute of Physics and Power Engineering (IPPE), Obninsk, Russia

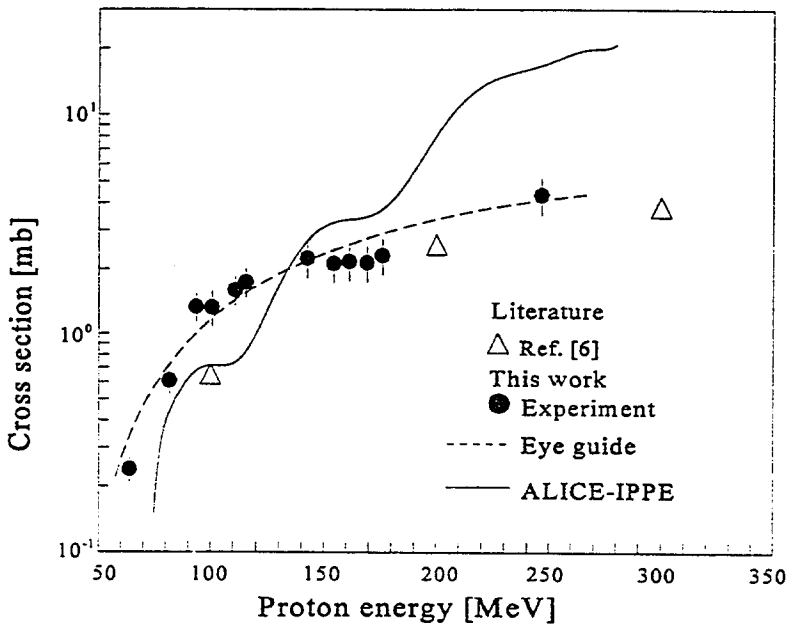

Fig. 2 Excitation function of ^{nat}Cl(p,x)^{22}Na process.

Using the measured data, the activation of beam collimators was estimated for a 30 min run of the therapy facility employing a 200 MeV proton beam with an intensity of 400 nA before collimation. Assuming two therapy runs on one week day, the various accumulated activities are given in Table 1. An estimate of the whole body dose rates at a distance of 1m from the source, caused by the activities accumulated in the collimator, was also carried out. Those results are also given in Table 1.

Table 1. Yearly produced radionuclide activity in brass collimators

Nuclide	**^{54}Mn**	**^{56}Co**	**^{57}Co**	**^{58}Co**	**^{65}Zn**
$T_{½}$[d]	312.2	78.8	271.3	70.8	244.0
A[MBq]	37.5	43.5	264.2	48.2	14.7
H_x[μSv/h]	4.8	5.6	12.8	7.2	1.2

Cross sections for the formation of ^{11}C from natural N and O were measured using AlN and SiO_2 as thin target materials for proton energies in the region 50 to 70 MeV and at 172 MeV. Nuclear model calculations were also done. For the $^{nat}N(p,x)^{11}C$ process extensive data existed up to 20 MeV. At higher energies the data base was weak. Worth mentioning is that two processes are involved, viz. $^{14}N(p,\alpha)^{11}C$ and $^{15}N(p,\alpha n)^{11}C$. The theory reproduced the shape of the excitation function to some extent [cf. 8].

Based on the present and literature data, an estimate of the radiation dose deposited by the short-lived positron emitters ^{11}C, ^{13}N and ^{15}O was done for liver as a source organ and a 200 MeV proton beam intensity of 5 nA/cm^2. The dose caused by these radionuclides amounts to approx. 500 mSv. Compared to a total radiation dose of 2 Sv per therapy run, the enhancement in the radiation dose through the decay of the short-lived β^+ emitters amounts to about 25%.

5. Excitation Functions Relevant to Radioisotope Production

A. Hohn, P. Reimer, A. Klein, Z. Kovács*, F. Tárkányi*, S.Takács*, A. Fenyvesi*, B. Scholten, H.H. Coenen, S.M. Qaim

In continuation of our systematic investigations on the cyclotron production of medically interesting radioisotopes [cf. 10, 11], we measured several excitation functions. The emphasis during the present report was on the β^+ emitters ^{51}Mn, ^{55}Co and ^{120}I, and on single photon emitters ^{57}Co and ^{99m}Tc.

Measurements relevant to the production of ^{51}Mn ($T_{½}$ = 46 min) were described in the last Progress Report. The ^{50}Cr(d,n)^{51}Mn process over the energy range $E_d = 9 \rightarrow 5$ MeV was found to be ideal. Now we investigated the ^{52}Cr(p,2n)^{51}Mn reaction from threshold to about 45 MeV. The cross section is very low and so this process is not suitable for production purposes.

^{55}Co ($T_{½}$ = 17.6 h) can be produced via ^{54}Fe(d,n)-, ^{56}Fe(p,2n)- and ^{58}Ni(p,α)-processes. The (p,2n) reaction is associated with large impurities and the (d,n) reaction has relatively low yield. Furthermore, the enriched target material ^{54}Fe is expensive. We therefore investigated the (p,x) reactions on highly enriched ^{58}Ni which is not very costly. Thin samples were prepared by electrolytic deposition of 99.9% enriched ^{58}Ni on Au foils and, after the irradiation, the radiocobalt was chemically separated. The measured excitation function of the reaction ^{58}Ni(p,α)^{55}Co depicted that the energy range $E_p = 15 \rightarrow 7$ MeV is suitable for the production of ^{55}Co. The rapid separation of radiocobalt after irradiation avoids the formation of the disturbing impurity ^{57}Co via the decay of ^{57}Ni. The level of ^{57}Co, however, cannot be reduced below 0.5%.

The nuclear data activities relevant to the production of ^{120g}I ($T_{½}$ = 1.35 h) were briefly mentioned in the last Progress Report. We now performed detailed excitation function measurements on the ^{122}Te(p,xn)^{122,121,120m,120g,119}I processes from their respective thresholds up to 45 MeV, using 97.1% enriched ^{122}Te as target material. The data for the ^{122}Te(p,3n)^{120m,g}I processes are given in Fig. 3 together with the preliminary

* Institute of Nuclear Research of the Hungarian Academy of Sciences (ATOMKI), Debrecen, Hungary

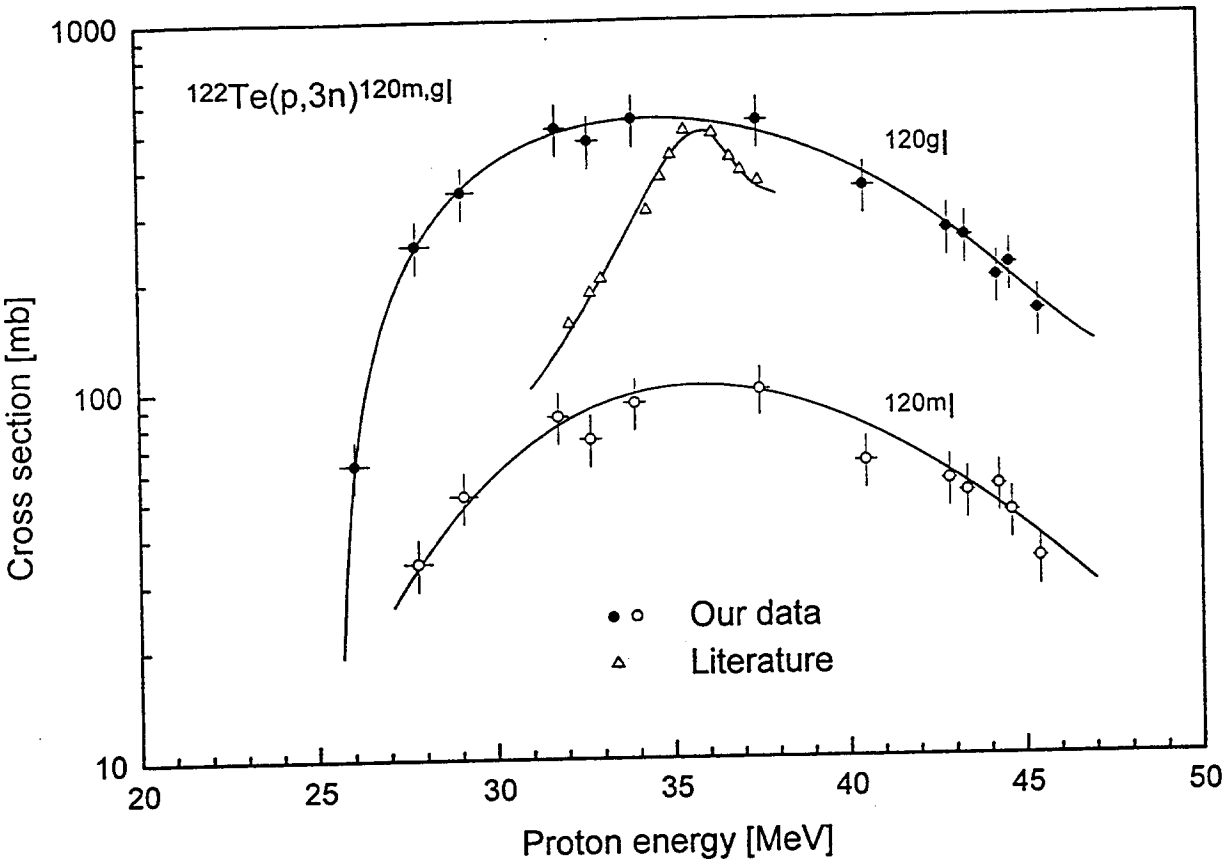

Fig. 3 Excitation functions of $^{122}Te(p,3n)^{120m,g}I$ processes. Whereas in this work individual contributions of ^{120m}I and ^{120g}I were resolved, the literature data deal with a mixture of the two isomers. The solid lines are eye-guides.

literature results (Zweit et al., 1995). We conclude that the literature data are incorrect, presumably due to the lack of analysis of the individual contributions of the two isomers (^{120}I and ^{120g}I). The work has been reported in detail elsewhere [12]. From the measured data the preferable energy range for the production of ^{120g}I is deduced to be $E_p = 37 \rightarrow 32$ MeV; its thick target yield amounts to 3.6 GBq (98 mCi)/μAh and the levels of ^{120m}I and ^{119}I impurities to 25 and 6%, respectively.

The nuclear data measurements relevant to the production of ^{99m}Tc ($T_{½}$ = 6.0 h) at a medium-sized cyclotron were completed. The implications of the data on production strategies are under review.

^{57}Co ($T_{½}$ = 271d) can be produced via the $^{58}Ni(p,2p)$-reaction. A radiochemical measurement of the excitation function revealed that this process has unexpectedly

high cross section. Over the optimum energy range of $E_p = 25 \rightarrow 15$ MeV, ^{57}Co can be produced in good yields and the level of ^{56}Co ($T_{½} = 79$ d) impurity is < 0.1%.

Besides the development work on the above mentioned radioisotopes, some cross section and product yield measurements on the nuclear processes $^{18}O(p,n)^{18}F$, $^{20}Ne(^3He,p)^{22}Na$, and $^{20}Ne(\alpha,d)^{22}Na$ were also performed. Part of the results have been published [13]; in other cases data analysis is in progress. Furthermore, some compilation and evaluation work on charged particle monitor reactions was also performed under a CRP of the IAEA [cf. 14].

References

[1] S. Merchel, S.M. Qaim: Excitation functions of (^3He,^7Be)-reactions on light mass target elements, Radiochimica Acta, in press

[2] S. Sudár, S.M. Qaim: Isomeric cross section ratio for the formation of $^{58m,g}Co$ in neutron, proton, deuteron and α-particle induced reactions in the energy region up to 25 MeV, Phys. Rev. C53 (1996) 2885

[3] C. Nesaraja, F. Cserpák, S. Sudár, R. Dóczi, S.M. Qaim: Excitation functions of (n,p) and (n,α) reactions on some isotopes of Zn, Ge, Y and Ag, Proc. Int. Conf. Nuclear Data for Science and Technology, Trieste, May 1997, in press

[4] B. Strohmaier, M. Faßbender, F.-O. Denzler, F. Rösch, S.M. Qaim: Isomeric cross section ratio for the formation of $^{94m,g}Tc$ in various charged-particle induced reactions, Proc. Int. Conf. Nuclear Data for Science and Technology, Trieste, May 1997, in press

[5] S.M. Qaim, F. Cserpák, J. Csikai: Excitation functions of $^{109}Ag(n,2n)^{108m}Ag$, $^{151}Eu(n,2n)^{150m}Eu$ and $^{159}Tb(n,2n)^{158}Tb$ reactions from threshold to 15 MeV, Appl. Radiat. Isotopes 47 (1996) 569

[6] S.M. Qaim, St. Spellerberg, F. Cserpák, J. Csikai: Radiochemical measurement of excitation function of $^{63}Cu(n,p)^{63}Ni$ reaction from 7.2 to 14.6 MeV, Radiochimica Acta 73 (1996) 111

[7] R.M. Klopries, R. Dóczi, S. Sudár, J. Csikai, S.M. Qaim: Excitation functions of some neutron threshold reactions on ^{89}Y in the energy range of 7.8 to 14.7 MeV, Radiochimica Acta 76 (1997) 3

[8] M. Faßbender, B. Scholten, Yu. N. Shubin, S.M. Qaim: Activation cross section data for (p,x) processes of therapeutic relevance, Proc. Int. Conf. Nuclear Data for Science and Technology Trieste, May 1997, in press

[9] M. Faßbender, Yu. N. Shubin, V.P. Lunev, S.M. Qaim: Experimental studies and nuclear model calculations on the formation of radioactive products in interactions of medium energy protons with copper, zinc and brass: Estimation of collimator activation in proton therapy facilities, Appl. Radiat. Isotopes, in press

[10] M.R. Zaman, S.M. Qaim: Excitation functions of (d,n) and (d,α) reactions on ^{54}Fe: relevance to the production of high purity ^{55}Co at a small cyclotron, Radiochimica Acta 75 (1996) 59

[11] B. Scholten, S. Takács, Z. Kovács, F. Tárkányi, S.M. Qaim: Excitation functions of deuteron induced reactions on ^{123}Te: relevance to the production of ^{123}I at low and medium sized cyclotrons. Appl. Radiat. Isotopes 48 (1997) 267

[12] A. Hohn, B. Scholten, H.H. Coenen, S.M. Qaim: Excitation functions of (p,xn)-reactions on highly enriched ^{122}Te: Relevance to the production of ^{120g}I, Appl. Radiat. Isotopes, in press

[13] A. Fenyvesi, S. Merchel, S. Takács, F. Szelecsényi, F. Tárkányi, S.M. Qaim: Excitation functions of ^{nat}Ne(3He,x)^{22,24}Na and ^{nat}Ne(α,x)^{22,24}Na processes: Investigation of production of ^{22}Na and ^{24}Na at a medium-sized cyclotron, Radiochimica Acta, in press

[14] S. Takács, M. Sonck, B. Scholten, A. Hermanne, F. Tárkányi: Excitation functions of deuteron induced nuclear reactions on ^{nat}Ti up to 20 MeV for monitoring deuteron beams; Appl. Radiat. Isotopes 48 (1997) 657

INSTITUT FÜR KERNPHYSIK
FORSCHUNGSZENTRUM JÜLICH

The Production Cross Section and the Lifetime of Heavy Λ Hypernuclei

H. Ohm[1], W. Borgs[1], W. Cassing[3], M. Hartmann[1], T. Hermes[1], L. Jarczyk[2], B. Kamys[2], H.R. Koch[1], P. Kulessa[2], R. Maier[1], D. Prasuhn[1], K. Pysz[1,2], Z. Rudy[2], H.J. Stein[1], A. Strzalkowski[2], O.W.B. Schult[1], Y. Uozumi[4], I. Zychor[5]

The (p,K) reaction on ^{238}U targets has been used at COSY Jülich to produce very heavy hypernuclei at projectile energies of 1.5 and 1.9 GeV [1,2]. These nuclei in which a Λ hyperon is bound in the nuclear potential were detected via fission induced by the decay of the Λ particle. Delayed fission fragments were identified in the background from prompt fission with the help of a recoil-shadow technique. Unambigious identification of fission fragments in the presence of a strong flux of minimal ionizingparticles like fast pions and protons was possible with two low-pressure multiwire proportional chambers which deliver time-of-flight and energy-loss information. In addition, the two-dimensional position information from the detectors was used to trace each particle back to a narrow region around the target. Thus the background sensitivity was reduced to a level of 10^{-7}.

The mean lifetime of the hypernuclei was deduced from the position distribution of fission events detected in the backward direction. In the analysis the forward recoil momentum of the hypernuclei is included which was taken from calculations based on the BUU approach [3]. The result is $\tau = 240 \pm 45(\text{stat.}) \pm 40$ (syst.) ps.

The cross section for the production of hypernuclei and their subsequent decay through the fission channel was determined from the event distribution in the shadow region and the prompt fission rate measured in the forward direction by normalizing to the prompt fission cross section of $\sigma =$ 1.5 b [4,5,6]. A value of $\sigma = (20 \pm 4\ (\text{stat.})\ ^{+13}_{-8}\ (\text{syst.})$ mb was obtained. From this value the total cross section for the production of hot hypernuclei prior to the evaporation of nucleons and the competing prompt fission was deduced with the help of calculations based on the BUU theory including statistical models [7]. The result is $\sigma = 200$ +- 40(stat.) $^{+130}_{-80}$ (syst.) mb. This value is in fair agreement with pedictions of 110 mb [7]. Analysis of data obtained with ^{209}Bi targets is in progress.

[1] Institut für Kernphysik, KFA Jülich
[2] Institute of Physics, Jagellonian University, Cracow, Poland
[3] Institut für Theoretische Physik, Universität Gießen
[4] Department of Nuclear Engineering, Kyushu University, Fukuoka, Japan
[5] Soltan Institute for Nuclear Studies, Swierk, Poland

References:

[1] T.Hermes et al., Proc. 3rd Int. Conf. Nucl.Physics at Storage Rings (STORI 96), to be published in Nucl. Phys. A
[2] H. Ohm et al., in print in Phys. Rev. C55 (1997), No.6
[3] Z. Rudy et al., Z. Phys. **A 351** (1995) 217
[4] J. Hudis, S. Katcoff, Phys. Rev. **C13** (1996) 1961
[5] B.A. Bogachov et al., Sov. J. Nucl. Phys. **28** (1978) 291
[6] L.A. Vaishnene et al., Z. Phys. **A 302** (1981) 143
[7] Z. Rudy et al., Z. Phys **A 354** (1996) 445

INSTITUT FÜR KERN- UND TEILCHENPHYSIK TECHNISCHE UNIVERSITÄT DRESDEN

1. Integral Activation Experiment with 14MeV Neutrons on Steels

H. Freiesleben, V. Kovalchuk*, D. Markovskij**, D. Richter, K. Seidel, V. Tereshkin*, S. Unholzer

Safety and environmental issues have increasing importance for the development of fusion power. Safety analyses of fusion reactor designs such as the International Thermonuclear Experimental Reactor (ITER) require among others a reliable data base for neutron-induced radioactivity. Extensive measured data were generated for about five years in the framework of a USDOE-JAERI collaborative programme [1]. Pure materials (V, Cu, Co, Ni, Mo, W and other) were irradiated in several neutron fields and the gamma activities induced were analysed with cross-section libraries and radioactivity codes available in the programme (ACT4, REAC-3, DKR-ICF, RACC). Summarizing the results the authors strongly advise to strengthen the endeavour in the area of integral measurements of induced radioactivity.

A joint effort of integral experiments has been started to validate the European Activation System (EAS) which has been adopted for the ITER design. It consists of the inventory code FISPACT [2] developed at Culham and of the European Activation File EAF-4 [3] compiled at Petten. In the neutron fields within the ITER inboard-shield mock-up at Frascati the activities induced in SS316 the structural material chosen for ITER are measured [4]. A white spectrum of fast neutrons ranging up to energies of 20MeV is used at Karlsruhe for irradiating low-activation steels such as MANET [5].

In the present work the activation of the same materials, i. e. MANET and the ITER SS316, with 14MeV neutrons is investigated. The irradiations were carried out at the high-intense neutron generator SNEG-13 [6] at Sergiev Posad. The 14MeV neutron fluence applied was monitored by the $^{93}Nb(n,2n)$ activation with a thin Nb foil attached to the steel samples. It was in the order of 10^{14} neutrons/cm^2. A possible background component of thermal neutrons was checked with a thin Au sample by $^{197}Au(n,\gamma)$ activation and found to be less than 3%. The time dependence of the neutron flux during the irradiation was recorded by integration of time intervals of 10min and taken into account in the calculations without any correction.

The samples had dimensions of 1cm * 1cm and a thickness of less than 1mm resulting in a mass of about 1g. The chemical composition is shown in Tbl. 1. The greatest difference is the reduced Ni content in MANET as compared to SS316. Also Cr, Mn and Mo are partly replaced by Fe.

Gamma spectra of the irradiated samples were recorded several times during cooling using conventional Ge(Li)-spectrometers. Gamma activities identified by energy and half-life were used to calculate the nuclide activities with gamma yield data of EAS. For the same cooling times the activities were calculated.

---

* Coordination Centre "Atomsafety", Sergiev Posad, Russian Federation
** Russian Research Centre "Kurchatov Institute", Moscow, Russian Federation

	SS316	MANET
Fe	65.42	86.76
Cr	17.7	10.3
Ni	12.1	0.62
Mn	1.77	0.94
Mo	2.29	0.56
V	0.09	0.20
Si	0.39	0.27
C	0.031	0.11
Nb	<0.05	0.15
N		0.030
Cu	0.09	0.007
As		0.010
Co	0.09	0.006
Al		0.006
P	0.023	0.005
S	0.002	0.004
B	0.0025	0.0089
Sn		0.001
Zr		0.009
Sb		0.0002
Pb	0.003	

Table 1: Elemental composition of the materials in w-%

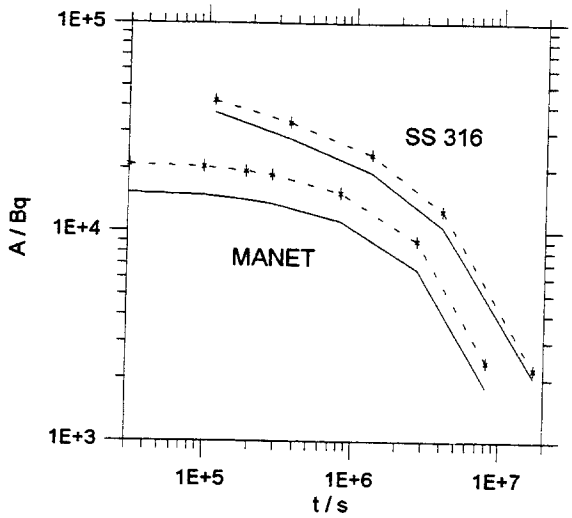

Fig. 1:

Sum of measured (dashed line) and calculated (solid line) activity of SS316 and MANET versus cooling time for a sample mass of 1.0g and a neutron fluence of 1.0 10^{14} neutrons/cm^2.

Activities of the following nuclides with half-life > 1d were measured and calculated: ^{48}Sc, ^{51}Cr, ^{54}Mn, ^{59}Fe, ^{57}Co, ^{58}Co, ^{60}Co, ^{57}Ni, ^{89}Zr, ^{92m}Nb, ^{95}Nb and ^{99}Mo. The largest half-life has ^{60}Co with 5.3a.

The sums of all activities identified are plotted in Fig. 1 as a function of the cooling time. They represent 90% of the total activity of gamma emitters at 1 d, 99% at 1 month and 99.9% at 1 a of cooling. Because they are normalized to equal sample mass and neutron fluence the activation behaviour of the two materials can be directly compared. The expected lower activation of MANET is observed. But in both cases the calculation underestimates the measured values. The dominating radionuclide for cooling times up to 1 month is ^{51}Cr which contributes about 80% to the activity of MANET and 50..60% to the SS316 activity. At 1 a cooling time to similar extent ^{54}Mn is dominating in MANET (^{57}Co on the second place) and ^{57}Co in SS316 (^{54}Mn on the second place). For these nuclides the experimental and calculated results are shown in Figs. 2 and 3. The experimental uncertainties include the uncertainties of the gamma spectroscopy, of the neutron fluence determination and of the gamma yield data and are about 7%. The largest underestimation is obtained for ^{51}Cr in both samples.

Tbl. 2 shows the pathways for the production of the dominating activities. There are two reactions which lead to ^{51}Cr in the 14MeV neutron field. Also with the white spectrum of fast neutrons used at Karlsruhe for irradiating MANET, a significant underestimation was found [5]. The different contributions of the two reactions in SS316 and in MANET (Tbl. 2) could indicate that the library cross section of the ^{54}Fe(n,α) is incorrect. Irradiating pure Fe samples in a fusion neutron field at FNS [1] an underestimation of this cross section with most of the data libraries used was stated. On the other hand in the shield mock-up at Frascati [4] good agreement of calculation and experiment was found for ^{51}Cr in SS316. But, in this bulk assembly there are additional contributions by thermal neutrons via the ^{50}Cr(n,γ) reaction. Certainly, also the ^{52}Cr(n,2n) cross section should be checked.

The conclusion from the results obtained so far is that the activation behaviour of MANET is better than that of SS316, as expected from calculations. The FISPACT/EAF-4 package reproduces the 12 activities dominating between 1 d and 1 a of cooling. No additional activities caused by unexpected impurities in the steels were found. The underestimations, especially of the activities listed in Tbl. 2, will be further analysed on the basis of the individual contributing reactions, with inclusion of the results obtained in other neutron fields.

Table 2: Results for the three activities dominating in the first year of cooling

Nuclide, half-life	Pathways	Contribution / % SS316	MANET	Calcul./Experim. SS316	MANET
^{51}Cr 27.70d	^{52}Cr(n,2n)	95.1	89.5	0.80	0.72
	^{54}Fe(n,α)	4.9	10.5		
^{57}Co 271.79d	^{58}Ni(n,d)	98.6	99.8	0.94	0.82
	^{58}Ni(n,2n)->β^{+},ε	together			
^{54}Mn 312.2d	^{55}Mn(n,2n)	56.8	52.2	0.95	0.88
	^{54}Fe(n,p)	42.6	47.1		
	^{56}Fe(n,t)	0.6	0.7		

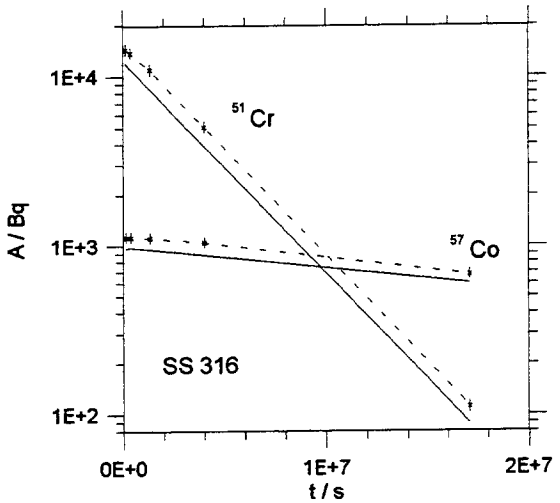

Fig. 2:

^{51}Cr and ^{57}Co activity versus cooling time as measured (dashed line) and calculated (solid line) for a SS316 sample of 1.0g of mass irradiated with a fluence of 5.95×10^{13} neutrons/cm^2.

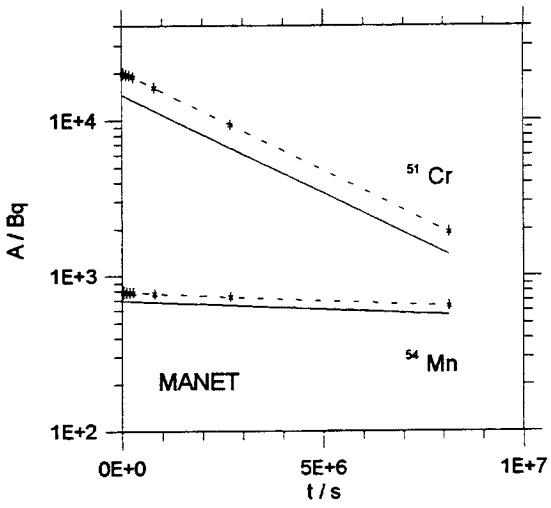

Fig. 3:

^{51}Cr and ^{54}Mn activity versus cooling time as measured (dashed line) and calculated (solid line) for a MANET sample of 0.8423g of mass irradiated with a fluence of 1.36×10^{14} neutrons/cm^2.

The TUD part of the work was supported by the European Fusion Technology Programme. The authors thank Dr. U. von Moellendorf and Dr. M. Pillon for supplying the MANET and SS316 samples, respectively.

References

[1] A. Kumar et al., Measurements of D-T neutron induced radioactivity in plasma-facing materials and their role in qualification of activation cross-section libraries and codes, Fusion Engrg. Des. 28 (1995) 596-609.
[2] R. A. Forrest and J-Ch. Sublet, FISPACT-4 - user manual, Report UKAEA FUS 287, Culham (1994).
[3] J. Kopecky and D. Nierop, The European Activation File EAF-4, Report ECN-C-95-072, Petten (December 1995).
[4] M. Pillon, M. Angelone and P. Batistoni, Measurement of the neutron induced activation in ITER grade AISI 316 LN, Report ENEA, Fusion Division, Frascati (November 1996).
[5] U. von Möllendorf, H. Giese and H. Tsige-Tamirad, Fusion materials activation tests with a deuteron-beryllium neutron source, Proc. 19th Symp. on Fusion Technology, Lisbon, 1996, to appear.
[6] V. D. Kovalchuk et al., Neutron generator SNEG-13; neutron and photon field characteristics, Report IAE-5589/8, Russian Research Centre "Kurchatov Institute", Moscow (1992).

2. Investigation of Spectral Neutron and Gamma Fluxes in a Fusion Reactor Blanket Mock-up

U. Fischer*, H. Freiesleben, W. Hansen, D. Richter, K. Seidel, S. Unholzer, Y. Wu*

The experimental validation of the nuclear performance of the shielding system is one of the tasks in the Engineering Design Activities for the International Thermonuclear Experimental Reactor (ITER). In a joint Japanese/US effort the outboard blanket is studied, whereas experiments dealing with the inboard shield are carried out by European and Russian groups [1]. The investigations of complex neutronics mock-ups started after detailed benchmarking [2] of the nuclear data libraries by experiments with simple geometry and homogeneous elemental materials.

The inboard shield mock-up includes first wall, blanket, vacuum vessel and toroidal field coils and was assembled at the Frascati Neutron Generator [3]. The Technical University of Dresden contributes to the joint programme [4] with measurements of neutron and gamma flux spectra in the mock-up. A reliable knowledge of these spectra is important for understanding neutron and gamma transport inside the assembly; furthermore they are the basic weighting functions for integral quantities such as reaction rates, nuclear heating, gas production and radiation damage.

The mock-up is shown in Fig.1. It consists of SS316 and Perspex slabs with dimension of 100cm*100cm and a total thickness of 94.3cm. Behind this block Cu and SS316 slabs are arranged simulating the coils for the toroidal magnetic field. The rear part of the assembly is surrounded with a polythene shield in order to reduce the background in this region. The neutronic equivalence to the ITER inboard shield was shown in pre-analyses.

---

* Forschungszentrum Karlsruhe, Institut für Neutronenphysik und Reaktortechnik, D-76021 Karlsruhe, Germany

Neutron and gamma spectra were measured on the central axis of the assembly at positions A and B [5]. Position A at a total penetration depth of z=41.5cm from the front slab corresponds to the back plate of the shield blanket. Position B at z= 87.6cm is close to the boundary of the vacuum vessel with the coils.

The measured neutron flux spectra are shown in Fig. 2 in comparison to calculated spectral fluxes. The calculations were carried out with the three-dimensional Monte Carlo code MCNP-4A [6] as coupled neutron-photon transport and with the ITER reference nuclear and atomic data library FENDL-1 [7]. The precise geometry of the mock-up as well as the complete surroundings (concrete walls of the building, metallic support of the assembly etc.) were taken into account. Also the energy-angle distribution of the 14MeV source neutrons was considered in detail.

With the exception of the lowest energy region the agreement is found to be good. The ratios of calculated-to-experimental fluxes integrated over energy ranges are presented in Tbl. 1. The uncertainties of the experimental values include both statistical and systematic errors. For the calculations only the statistical uncertainty of the Monte Carlo run is indicated; data errors are not included. For position A the agreement is within an interval of 10 - 15%. For position B a slightly increased underestimation is observed.

Comparisons of the measured gamma fluxes with calculated ones are shown in Fig. 3 and Tbl. 2. An overall good agreement can be stated and also the tendency of a slight underestimation with penetration depth. That is in agreement with findings of a bulk shielding experiment at JAERI analysed with MCNP and the Japanese Evaluated Nuclear Data Library, Version 3 [8].

The good consistency with integral data measured at the mock-up by other groups allowed to derive values of nuclear design parameters such as gas production, heating and damage for the two positions of spectral measurements [9].

Table 1: Comparison of measured and calculated neutron fluences for different energy ranges per one source neutron at position A (upper part) and position B (lower part)

E / MeV	0.1 - 1.0	1.0 - 5.0	5.0 - 10.	10. - 15.	0.1 - 15.
Experiment / cm^{-2}	$2.76\ 10^{-6}$ $\pm 0.28\ 10^{-6}$	$1.43\ 10^{-6}$ $\pm 0.08\ 10^{-6}$	$2.47\ 10^{-7}$ $\pm 0.13\ 10^{-7}$	$5.43\ 10^{-7}$ $\pm 0.14\ 10^{-7}$	$4.98\ 10^{-6}$ $\pm 0.41\ 10^{-6}$
Calculation / cm^{-2}	$2.39\ 10^{-6}$ $\pm 0.03\ 10^{-6}$	$1.28\ 10^{-6}$ $\pm 0.02\ 10^{-6}$	$2.56\ 10^{-7}$ $\pm 0.09\ 10^{-7}$	$4.88\ 10^{-7}$ $\pm 0.18\ 10^{-7}$	$4.42\ 10^{-6}$ $\pm 0.04\ 10^{-6}$
Calc./Exp.	0.86±0.09	0.90±0.05	1.04±0.07	0.90±0.04	0.89±0.08
E / MeV	0.1 - 1.0	1.0 - 5.0	5.0 - 10.	10. - 15.	0.1 - 15.
Experiment / cm^{-2}	$8.78\ 10^{-9}$ $\pm 0.89\ 10^{-9}$	$2.37\ 10^{-9}$ $\pm 0.13\ 10^{-9}$	$2.69\ 10^{-10}$ $\pm 0.14\ 10^{-10}$	$5.79\ 10^{-10}$ $\pm 0.15\ 10^{-10}$	$1.20\ 10^{-8}$ $\pm 0.10\ 10^{-8}$
Calculation / cm^{-2}	$6.00\ 10^{-9}$ $\pm 0.08\ 10^{-9}$	$1.81\ 10^{-9}$ $\pm 0.04\ 10^{-9}$	$2.93\ 10^{-10}$ $\pm 0.15\ 10^{-10}$	$4.56\ 10^{-10}$ $\pm 0.25\ 10^{-10}$	$8.56\ 10^{-9}$ $\pm 0.09\ 10^{-9}$
Calc./Exp.	0.68±0.07	0.76±0.04	1.09±0.08	0.79±0.05	0.71±0.09

Table 2: Comparison of measured and calculated gamma fluences for E > 0.4MeV per one source neutron

E > 0.4 MeV	Position A	Position B
Experiment / cm^{-2}	(7.47±0.19) 10^{-6}	(1.07±0.03) 10^{-8}
Calculation / cm^{-2}	(7.63±0.15) 10^{-6}	(9.55±0.28) 10^{-9}
Calc./Exp.	1.02±0.03	0.89±0.04

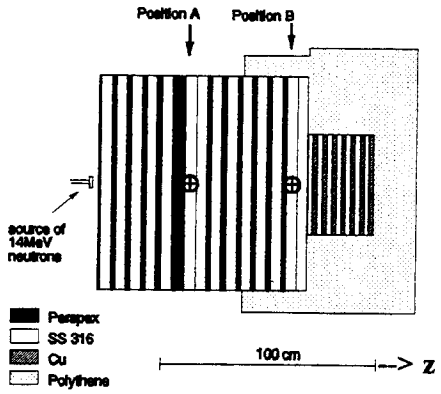

Fig. 1:
Inboard-shield mock-up and positions of neutron and gamma flux spectra measurements.

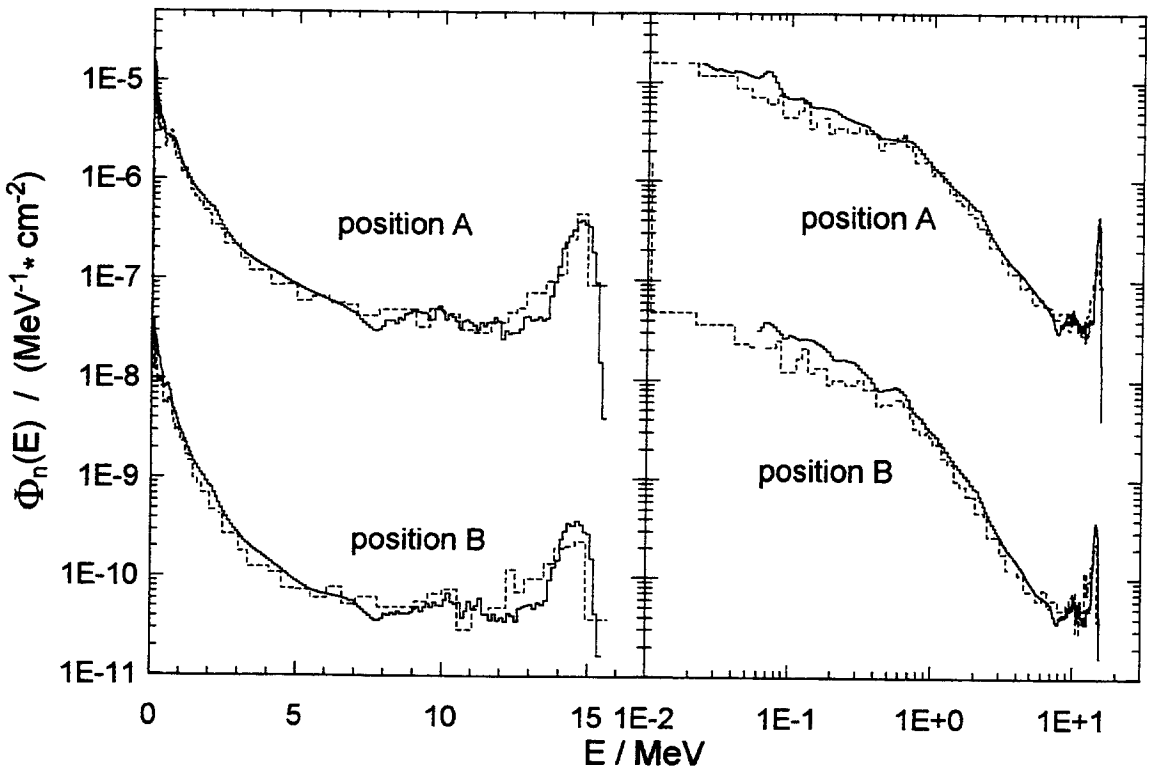

Fig. 2: Neutron fluences per one source neutron measured (solid line) and calculated (dashed line) at positions A and B versus logarithmic (right hand side) and linear (left hand side) energy scale.

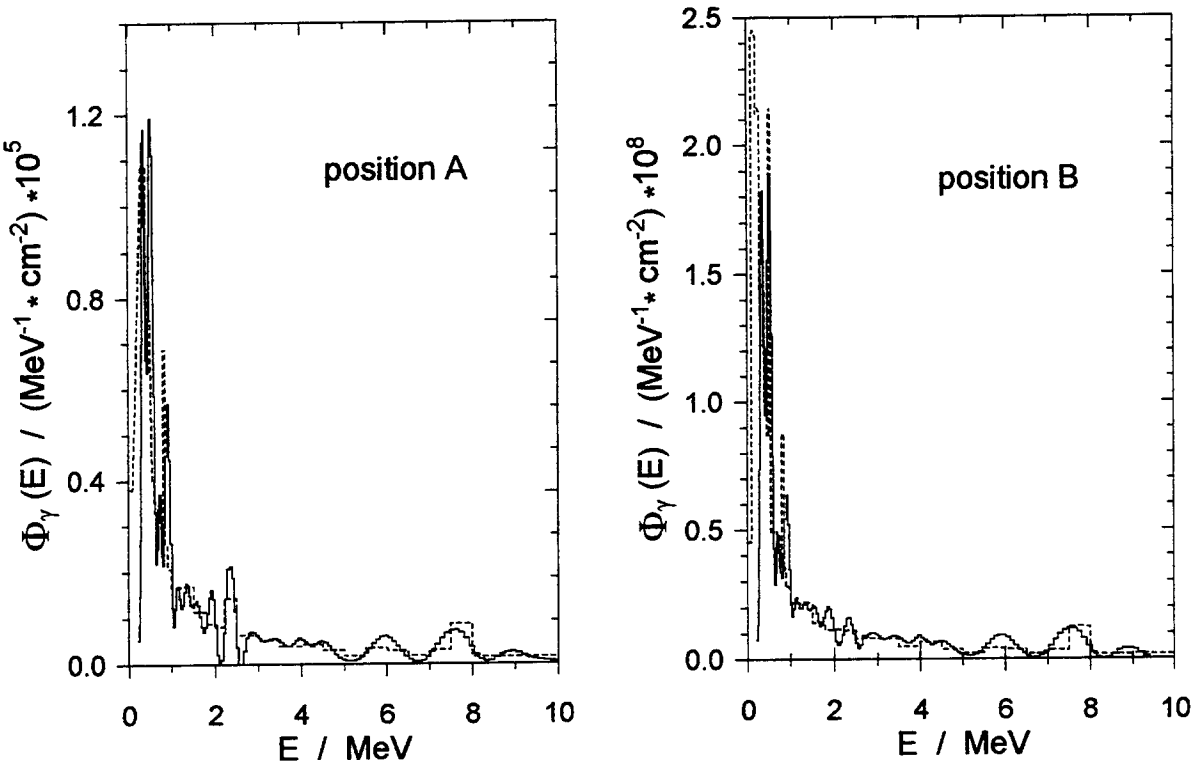

Fig. 3: Gamma fluences per one source neutron measured (solid line) and calculated (dashed line) at positions A (left hand side) and B (right hand side) versus energy.

Work supported by the European Fusion Technology Programme

References

[1] R. Santoro, T-218 Meeting on "Shielding Neutronics Experiments", Frascati, March 1-2, 1995.

[2] U. Fischer (ed.), Integral data tests of the FENDL-1 nuclear data library for fusion application, Report Forschungszentrum Karlsruhe, FZKA 5785, INDC(GER)-41 (August 1996).

[3] M. Martone, M. Angelone and M. Pillon, The 14 MeV Frascati neutron generator, Journal of Nuclear Materials, 212 (1994) 1661-1664.

[4] P. Batistoni et al., Neutronics shield experiment for ITER at the Frascati neutron generator FNG, Proc. 19th Symposium on Fusion Technology, Lisbon, 1996, to appear; Book of Abstracts, page 32.

[5] H. Freiesleben et al., Measurement of spectral neutron and photon fluxes in an ITER blanket mock-up, Progress Report on Nuclear Data Research in the Federal Republic of Germany, ed. by S. M. Qaim, NEA/NSC/DOC(96)24, INDC(GER)-042, p. 18, Jülich 1996.

[6] J. F. Briesmeister, MCNP - a general Monte Carlo n-particle transport code, version 4A, Report LA-12625-M, Los Alamos (September 1993).

[7] S. Ganesan and P. K. McLaughlin, FENDL/E - evaluated nuclear data library of neutron interaction cross-sections and photon production cross-sections and photon-atom interaction cross-sections for fusion applications, version 1.0, Report IAEA-NDS-128, Vienna (May 1994).

[8] F. Maekawa et al., Bulk shield experiment on a large SS316/water assembly bombarded by d-t neutrons, Report JAERI 95-018 (March 1995).

[9] H. Freiesleben et al., Neutron and photon flux spectra in a mock-up of the ITER shielding system, 4th International Symposium on Fusion Nuclear Technology, Tokyo, April 6-11, 1997

3. Self-Ionization Probabilities after K-Shell Ionization

A. El-Shemi*, G. Zschornack

Inner-shell ionization processes were analyzed under different points of view. Thereby, basic investigations of atomic properties as well as investigations in connection with other disciplines as solid state physics, plasmaphysics and astrophysics were of interest. Here we tract atomic reorganization cascades following inner-shell vacancy production and the creation of multiply ionized atoms connected with it. The importance of this process is based on the fact, that because of atomic reorganization cascades ionized atoms with different ion charge states are produced, e.g., as result of a primary inner-shell vacancy ions with different charge states can be created.

Atomic reorganization starts by filling the initially created vacancy either by a radiative transition (X-rays) or by an Auger process. New vacancies created during this atomic reorganization may in turn be filled by further radiative and non-radiative transitions until all vacancies reach the outermost occupied shells (energetically stable final states or metastable ones because of relevant selection rules). In the case of X-ray processes the vacancy moves to an outer shell under emission of characteristic X-rays, while for non-radiative transitions one electron from an outer shell fills up the inner-shell vacancy and another electron is ejected into the continuum. With exception of the K and L shells of heavy atoms, Auger processes are much more probable than X-rays and since an electron is ejected in each Auger process, a series of such events, called vacancy cascade, gives rise to a highly charged ion.

The investigation of vacancy cascades has been of considerable interest in different fields of research. Thus, thermal multicharged ions can be produced on intensive sources of synchrotron radiation by sequential K-shell photoionization and following vacancy cascades [1, 2, 3, 4]. The so produced thermal ions allow fundamental investigations on the collision physics in different plasmas as well as precision spectroscopy for testing QED effects and quantummechanical electron transfer theories. Vacancy cascades in large molecules leading to molecule decomposition (molecule fragmentation) [5, 6, 7, 8]. Corresponding investigations are also of importance for understanding material damages after irradiation and for understanding detection mechanisms of ionizing radiation. For investigations of solid state effects at photoelectron emission, electron-loss spectroscopy and for EXAFS the energy dependence of the resulting charge spectrum from the excitation energy near the absorption edges is of importance [9, 10, 11].

Here we calculate the probabilities $P(q)$ that q-fold ionized atoms are produced after a primary inner-shell ionization of neutral atoms. The computer code developed for this purpose [12, 13] allows to use different atomic data published in the literature. For systematic investigations the problem occurs, that most of the elements consistent sets of atomic data are not available. Therefore, we calculate radative transition probabilities with a computer code developed by Reiche [14] using MCDF wave functions [15, 16] and non-radiative transition probabilities with a code written by Lorenz and Hartmann [17]. Shake-off probabilities were calculated with an own computer code [18]. Beside shake-off processes the closing of energetically forbidden Coster-Kronig channels during the cascade development is considered. A more detailed description of the calculation is given in [19].

The localization of a primary vacancy decisively determines the development of a vacancy cascade. Deeper vacancies lead to higher mean ion charge states and vacancies in outer shells produce only ions with some few additional vacancies because of the restricted number of possible deexcitation channels.

---

* Department of Physics, El-Minia University, 61111 Minia, Egypt

The deexcitation of a primary K-shell vacancy in neon occurs with high probability by KLL Auger transitions because of the small K fluorescence yield (ω_K(Ne) = 0.015 [20]). As a result of this KLL transition the contribution of Ne^{2+} ions is 77.4%. New vacancies created by this process could not further deexcite by non-radiative electron transitions, e.g. Ne3+ and Ne4+ ions are produced exclusively by electron shake-off processes. Generally we find this situation for the production of primary vacancies in the outermost subshells, where non-radiative deexcitation processes are impossible.

Ion charge state distributions for the deexcitation of primary neutral atoms after K-shell ionization are presented in Table 1 for the atomic number region from Z=10 to Z=60. Results for Z=76 and Z=80 are added.

Table 1: Ion charge state distributions (in percent) for different neutral atoms after deexcitation of a primary K-shell vacancy. Tabulated are contributions greater than 0.1%. q - final ion charge

q	Z=10	Z=12	Z=14	Z=16	Z=18	Z=19	Z=20	Z=22	Z=24	Z=25	Z=26	Z=30
1	1.0			0.2	0.5	0.5						0.2
2	77.4	3.1	1.0	4.4	7.1	4.0	1.6	1.8	2.6	3.0	4.2	7.4
3	20.8	60.5	4.2	7.0	10.1	9.4	10.2	2.4	4.8	5.1	6.8	14.8
4	0.9	27.1	46.3	33.1	35.4	16.8	11.0	16.0	13.7	10.0	10.5	16.2
5		7.3	40.8	33.1	33.7	40.4	30.5	19.3	16.8	13.1	12.3	17.7
6		1.8	6.3	20.0	10.9	24.5	32.9	35.8	10.1	17.3	12.7	20.2
7		0.2	1.2	2.1	1.9	4.1	10.3	19.0	27.5	17.7	17.9	14.1
8			0.1	0.1	0.3	0.3	3.3	4.8	19.0	22.2	18.8	2.8
9							0.2	0.8	4.6	9.1	12.6	2.8
10								0.1	0.7	2.3	3.7	2.1
11											0.4	1.7
q	Z=34	Z=36	Z=37	Z=38	Z=40	Z=44	Z=48	Z=50	Z=54	Z=60	Z=76	Z=80
1	0.3	0.4	0.4	0.4	0.1	0.2	0.1	0.6	0.2	0.2	0.1	0.4
2	0.8	0.9	0.8	0.6	0.6	1.4	1.7	2.1	1.9	0.6	0.6	1.0
3	3.7	3.7	3.3	1.8	1.1	2.7	3.1	4.2	1.1	2.3	1.0	1.6
4	23.7	18.9	10.6	7.3	5.4	5.7	7.5	8.4	4.3	4.2	2.2	7.9
5	31.7	21.1	17.3	18.2	14.8	11.9	13.1	12.0	5.8	6.6	4.2	5.8
6	28.5	17.4	15.1	16.0	19.1	15.2	15.3	13.7	11.4	10.6	8.6	9.2
7	9.5	12.8	14.1	14.7	15.4	15.9	14.6	13.1	14.3	15.2	11.5	5.7
8	1.4	9.9	10.2	11.8	12.5	11.6	5.8	11.0	18.9	25.3	5.1	8.9
9	0.2	7.0	9.2	7.6	9.5	12.8	7.7	9.1	14.2	15.0	8.6	8.5
10		5.0	10.5	10.0	7.9	7.5	7.1	7.0	9.3	7.6	10.5	4.0
11		2.2	5.8	7.1	6.9	5.6	5.7	5.0	5.9	1.7	11.2	6.9
12		0.7	2.0	3.1	4.9	5.2	6.5	3.8	3.8	2.4	11.4	6.3
13			0.5	1.0	1.5	3.1	4.9	3.1	2.9	1.8	9.7	7.3
14			0.1	0.2	0.3	1.0	3.4	3.3	2.2	1.7	7.2	6.9
15						0.2	2.1	2.1	1.6	1.6	4.1	6.9
16							1.0	1.0	0.9	1.2	1.8	5.2
17							0.3	0.3	0.2	0.9	0.9	3.1
18										0.5	0.5	2.4
19										0.3	0.3	1.0
20										0.1	0.2	0.7
21											0.1	0.1

Generally, the mean ion charge state after the deexcitation of inner-shell vacancies increases with increasing atomic number because of the increasing complexity of the atomic structure and the increasing number of possible non-radiative transitions. Thus, for very complex atoms it is less probable to find atoms with low charge states q after deexcitation processes.

In atoms up to neon the creation of a K-shell vacancy is with high probability followed by Auger KLL transitions. In this case a double ionized atom is produced. Higher ionized light atoms arise from electron shake-off processes. Beginning with sodium, besides KLL Auger transitions KLM and LLM transtions appear during the cascade deexcitation, e.g., higher ionized atoms become more probable. The non-monotonous behavior of the derived ion charge state spectra and mean ionization stages are referred to the fact, that with increasing atomic number and changes in the occupation of atomic shells new Coster-Kronig channels are opened or appear to be forbidden.

For K-shell deexcitation an increasing broadening of the resulting ion charge state distribution appears due to the increasing complex atomic structure and the deexcitation channels connected with it.

An overview on ion charge state distributions in the course of cascading deexcitation of atomic inner-shell vacancies in the K-shell is given. Charge multiplying vacancy cascades are analyzed for primary singly ionized free atoms. Calculation results show a permanent increase of the number of ejected electrons with increasing complexity of the atomic structure. Thus, for high-Z atoms single ionization in atomic inner-shells is a possible method to create alternative to high-energetic collision processes highly charged ions without high momentum transfer.

References

[1] D. A. Church et al.; J.Phys., B17 (1984) L401
[2] D. A. Church et al.; Phys. Rev. Letter, 56 (1986) 2614
[3] D. A. Church et al.; Physical Review, A36 (1987) 2484
[4] K. W. Jones, B. M. Johnson, M. Meron; Phys. Lett., 97A (1983) 377
[5] T. A. Carlson, R. M. White; J. Chem. Phys., 44 (1966) 4510
[6] T. A. Carlson, R. M. White; J. Chem. Phys., 48 (1968) 5191
[7] U. Kyoshi et al.; Physics Letters, 154 (1989) 357
[8] U. Kyoshi et al.; Physica Scripta, 41 (1990) 67
[9] T. B. Hastings, V. O. Kostroun; Nuclear Instruments & Methods, 208 (1983) 815
[10] T. Hayaishi et al., J.Phys., B17 (1984) 3511
[11] T. Tonuma et al., J.Phys., B20 (1987) 4453
[12] A. M. M.Mohammedein et al.; Radiation Effects and Defects in Solids, 126 (1993) 309
[13] A. M. M. Mohammedein; Doctor Thesis, TU Dresden, Fakultät für Mathematik und Naturwissenschaften, Dresden, 1994
[14] I. Reiche; Doctor Thesis, TU Dresden, Fakultät für Mathematik und Naturwissenschaften, Dresden, 1992
[15] I. P. Grant et al.; Comp. Phys. Commun., 21 (1980) 207
[16] B. J. McKenzie, I. P. Grant, P. H. Norrington; Comp. Phys. Commun., 21 (1980) 233
[17] M. Lorenz, E. Hartmann; Report ZfI-109, Leipzig 1985, p.27
[18] A. M. El-Shimy, G. Zschornack; Progress Report on Nuclear Data Research in the Federal Republic of Germany for the Period April 1, 1993 to March 31, 1994, ed. by S. M. Qaim, NEA/NSC/DOC(94)21, INDC(Ger)-039/LN, Jül-2950, Jülich, 1994, p.29
[19] A. El-Shemi, Y. Lofty, G. Zschornack; J.Phys., B30 (1997) 237
[20] W. Bambynek; Proc. Int. Conf. on X-Ray and Inner-Shell Processes in Atoms, Molecules and Solids, August 20-24, 1984, Leipzig, Post-Deadline Abstracts, p.1

4. Measurement of L X-ray intensity ratios for electron excitation in the atomic number region Z = 47 to 74

D. Küchler, J. Tschischgale, G. Zschornack

For application in X-ray spectral analysis, molecule physics, solid state physics and for material investigations an exact knowledge of the intensity ratios between different X-ray lines is required.

Although in the literature the intensity of an X-ray line is given as $h\nu \cdot n$ ($h\nu$: photon energy; n: number of detected quanta per time and area), usually the ratio of the registered events is understood as intensity ratios. In calculations this problem becomes gone around when as intensity ratios the ratio of the calculated emission rates is taken into account. Here we define as intensity ratio the number of detected events for peaks corresponding to different X-ray transitions.

From previously published literature on intensity ratio data of L X-ray lines in the atomic number region Z = 47 until Z = 74 is known, that the intensity ratios (L_l/L_α, $L_{\beta 1}/L_\alpha$ and $L_{\gamma 1}/L_{\beta 1}$) calculated by several authors (Scofield [1, 2], Salem [3, 4] and Reiche [5]) are different up to a factor 4 from one another.

Measurements in the interesting atomic number region were carried out by Wyckoff [6], Raghavaiah [7] and Salem [8]. Their results also strongly scatter. Complete data files, derived by only one author over the observed atomic number region are practically not available.

To close the existing data gaps, measurements of the intensity ratios of L X-ray series were carried out with solid state targets after excitation by electrons using a Si(Li) semiconductor detector. Special attention was paid to the determination of intensity ratios in the rare earths region.

The $L_{\alpha 1,2}$-, $L_{\beta 1}$-, $L_{\beta 2}$-, $L_{\gamma 1}$-, $L_{\gamma 2,3}$- and the L_l- lines were evaluated [9]. The measured peaks were corrected for:

1. Self-absorption and matrix effects in the thick target because radiation is produced not only at the target surface and therefore radiation losses appear.
2. Energy dependence of the detection efficiency that is strong in the energy region of rare earths X-rays. A calibration method was developed to determine the relative detection efficiency in the low energy region [10]. This calibration is based on energy dispersive measurements of electron bremsstrahlung emitted by an X-ray tube. Thick-target model bremsstrahlung spectra were computed in a semiclassical approximation and from a physical based model of the detector response. Then in the next step the model spectra were fitted to the measured spectra. Thereby, the uncertainty of the detector efficiency is about 5%.

In Fig. 1 measured $L_{\beta 1}/L_\alpha$ intensity ratios are presented as an example. The measurements fill up the area of the rare earths that was only incompletely analyzed before. The experimental data correspond to the results of other authors. The experiments carried out confirm the situation observed already in earlier experiments that in contrast to the K X-ray series intensity ratios were calculated only partly for the L series with sufficient precision. All published calculations refer to free atoms. Calculations in the solid state depend sensitively on the realized electron distribution and can influence intensity ratios over a wide area. It should be mentioned that all data to be used for comparison result from thick target conditions what is also the case in the majority of X-ray fluorescence applications.

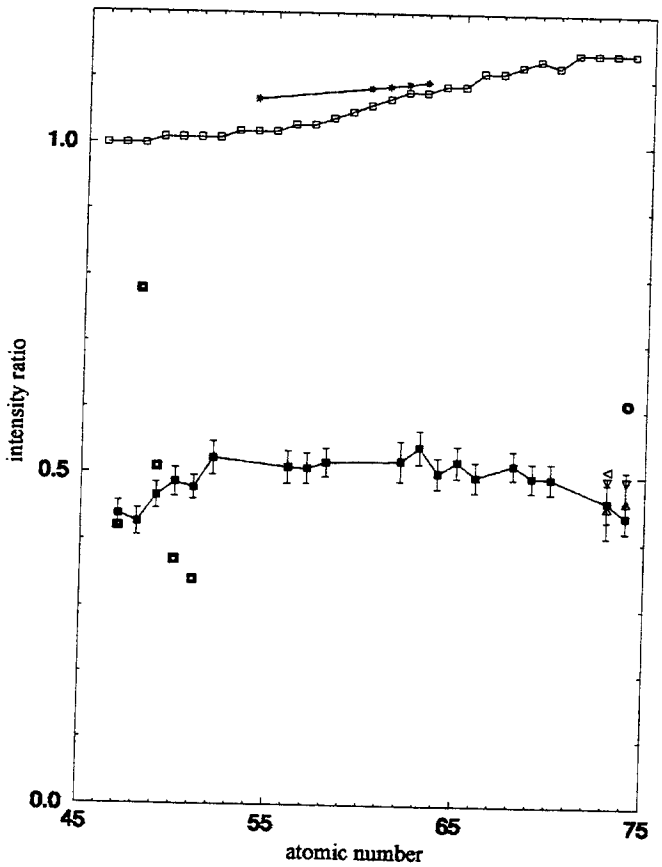

Fig. 1: Intensity ratio $L_{\beta 1}/L_{\alpha}$ as a function of the atomic number Z. The experimental values shown are from Andrew (▽, [11]), Goldberg (△, [12]), Hicks (◁, [13]), Victor (○, [14]) and Wyckoff and Davidson (boldfaced □, [6]) as well as calculated MCDF values of Reiche (*, [5]) and results of Dirac-Hartree-Slater-calculations of Scofield (□, [1, 2]). Own results are labeled with ■.

References

[1] J. H. Scofield; Physical Review, 10 (1974) 1507

[2] S. T. Perkins et al.; Tables and Graphs of Atomic Subshell and relaxation dates Derived from the LLNL Evaluated Atomic Data Library (EADL) Z=1-100, UCRL-504000, Vol.30, Livermore, 1991

[3] S. I. Salem, C. W. Schultz; Atomic Data, 3 (1971) 215

[4] S. I. Salem, S. L. Panossian, R. A. Krause; Atomic Data and Nuclear Data Tables, 14 (1974) 91

[5] I. Reiche; Diplomarbeit, TU Dresden, Sektion Physik, Dresden, 1988

[6] R. W. Wyckoff, F. D. Davidson; Journ. of Appl. Physics, 6 (1965) 1883

[7] C. V. Raghavaiah et al.; X-Ray Spectroscopy, 19 (1990) 23

[8] S. I. Salem, R. T. Tsutsui, B. A. Rabbani; Physical Review, A4 (1971) 1728

[9] J. Tschischgale, Diplomarbeit, TU Dresden, Institut für Kern- und Teilchenphysik, Dresden, 1997

[10] J. Tschischgale, D. Küchler, U. Lehnert, G. Zschornack; submitted to Nuclear Instruments & Methods

[11] V. J. Andrew; Physical Review, 42 (1932) 591

[12] M. Goldberg; Ann. der Physik, 7 (1962) 329

[13] V. Hicks; Physical Review, 38 (1931) 572

[14] C. Victor; Ann. Phys. (Paris), 6 (1961) 183

ABTEILUNG NUKLEARCHEMIE
UNIVERSITÄT ZU KÖLN
AND
ZENTRUM FÜR STRAHLENSCHUTZ UND RADIOÖKOLOGIE
UNIVERSITÄT HANNOVER

1. A New Facility at the The Svedberg Laboratory for Parasitic Activation Experiments with Medium-Energy Neutrons

S. Neumann[1], R. Michel[1], O. Jonson[2], P. Malmborg[2], F. Sudbrock[3], U. Herpers[3], B. Holmqvist[4]

Cross sections for the production of residual nuclides by medium-energy neutrons are high-priority data in many fields of applications ranging from accelerator technology over space and aviation technology, medical applications, radiation protection to geo- and cosmophysics. However, in spite of their importance neutron cross sections for energies above 14 MeV are scarce. There are just few facilities available which allow to activate targets with quasi-monoenergetic medium-energy neutrons. Most of them have the problem of too low neutron flux densities to perform activation experiments in a reasonable experiment time.

In order to improve this situation, a new facility was built and installed at the neutron beam line [1] of the The Svedberg Laboratory during autumn 1996. This neutron irradiation facility is situated about 1.7 m downstream the neutron production target (99.984 % ^{7}Li) in the Marble Hall and makes use of protons produced at an angle between 0.8° and 1.6° off the beam-axis. At this position, after the bending magnet which removes the primary protons and just before a narrow revolver-collimator, this facility does not interfere with other neutron experiments going on in the Blue Hall further downstream and experiments can be done in a fully parasitic mode. It allows for long-term neutron activation of targets with diameters up to 25 mm and a length of 60 mm. The targets to be irradiated are handled by a pneumatic tube system where a shuttle (rabbit) containing the targets can be transported from an uncleared area to a remotely driven pneumatic elevator below the beam pipe. A thin aluminum wall separates the beam-line vacuum from the irradiation chamber where the targets are in air.
Relative neutron beam intensities are logged on-line. Neutron energies up to 100 MeV can be obtained with flux densities in the high-energy peak of about $0.5 \cdot 10^{5}$ cm^{-2} s^{-1} μA^{-1} (mm Li)$^{-1}$, which is about a factor of 40 more than obtainable in the Marble Hall. Lithium targets up to 10 mm thickness and proton currents up to 6 μA can be used in this beam line. Above 100 MeV, neutrons up to 180 MeV can be obtained, but with flux densities about one order of magnitude lower.

[1]Zentrum für Strahlenschutz und Radioökologie, Universität Hannover, F.R.G.
[2]The Svedberg Laboratory, University of Uppsala, Sweden
[3]Abteilung Nuklearchemie, Universität zu Köln, F.R.G.
[4]Department of Neutron Research at Studsvik, University of Uppsala, Sweden

After a successful test experiment with a preliminary setup [2], which demonstrated the feasibility of this approach, first experiments were performed with 3 μA proton beams of 78.1 ± 0.2 MeV and 97.5 ± 0.3 MeV irradiating 4 mm and 8 mm Li targets, respectively. The homogeneity of the neutron flux inside the irradiation chamber as well as the background of thermal and epithermal neutrons and of secondary protons was investigated. The neutron flux density was found to be constant over the cross section of the shuttle within the limits of statistical errors (4 %) of the measurements. The gradient of the neutron flux density inside the shuttle can be explained by the inverse quadratic dependence of the flux density on the distance from the Li-target and by nuclear attenuation due to the irradiated targets. No evidence for change of the neutron spectrum inside the shuttle could be found from the analysis of reactions with Q-values between 1.71 MeV and -51.2 MeV. Flux densities of secondary protons are lower than those of the medium-energy neutrons by a factor of about 10^{-3}.

Up to ten target elements (C, Al, Si, O as quartz, Fe, Co, Ni, Cu, Ag, and Pb) were irradiated for up to 69.4 h (including interruptions). After irradiation, γ-spectrometry was immediately started. Short-lived radionuclides with half-lives between 20 min and a few hours were measured with good precision. γ-spectrometry was continued in Hannover to measure long-lived nuclides with half-lives up to 5 years. Later on, C, Al, Si and quartz targets are chemically processed and Be-10 and Al-26 are separated for measurement by accelerator mass spectrometry (AMS) at the PSI/ETH Tandem AMS facility at Zürich. The feasibility of such analyses was meanwhile demonstrated using the targets from the first test experiment [2]. The entire measurements demonstrate that the experimental conditions at the new irradiation device at TSL allow to determine activation cross sections by medium-energy neutrons for all radionuclides of interest independent of their half-lives.

From each irradiation spectrum-weighted cross sections are obtained. An example is given in fig. 1 for the target element copper. The experimental responses were normalized to a flux density which was constructed using kinematic calculations for the high-energy peak and information for the low energy spectrum from earlier reconstructions of the spectrum [1]. Absolute normalization was obtained from the experimentally measured ^{105}Ag response by using this spectrum and Ag(n,xn)^{105}Ag cross sections [3].

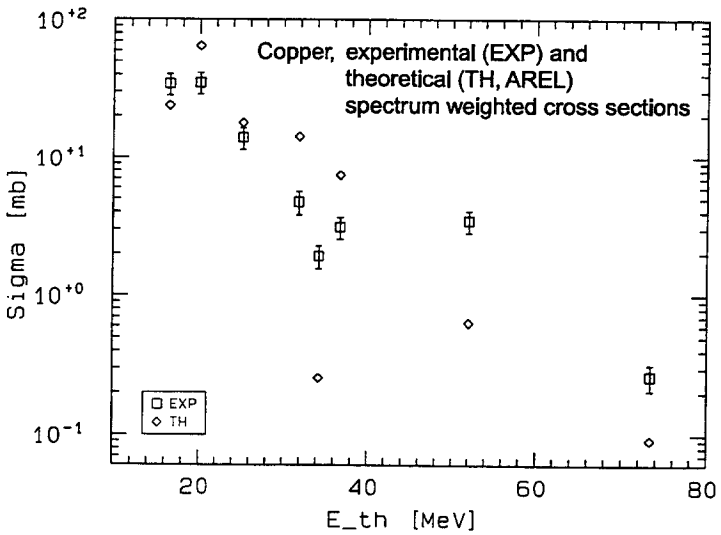

Fig. 1 *Spectrum-weighted cross sections for the target element copper versus the thresholds of the reactions compared with theoretical cross sections calculated by the AREL code.*

The spectrum-weighted cross sections allow to determine the excitation functions by making an energy- dependent least squares adjustment [5]. Integral excitation functions will be extracted after having done a number of irradiation experiments covering peak energies over a wide energy range. The experimental spectrum-weighted cross

sections (Fig. 1) show a decrease with increasing threshold. They are compared with theoretical ones calculated by the hybrid model of preequilibrium reaction in the form of the AREL [4] code. Reasons for the observed discrepancies can be wrongly calculated thresholds, not accounting for preequilibrium α-emission in the AREL code and also an erroneous differential flux density.

Presently, all activities are measured relative to those induced in the target element copper which is an ideal and inexpensive monitoring target element. Work is underway to establish monitor excitation functions for copper by absolute determinations of the neutron fluence and the differential flux density. For energies below 70 MeV, these monitor cross sections will then be connected to existing medium-energy cross sections for the target element silver [3]. It is planned to do the absolute measurements of the neutron fluence and the differential neutron flux density inside the shuttle by fission break-down detectors or ^{238}U fission chambers and to connect these measurements to the (n,p) cross section as a primary standard.

References:

[1] H. Condé et al., Nucl. Instr. Meth. Phys. Res. **A292** (1990) 121

[2] S. Neumann et al., TSL Annual Report 1994 - 1995 (1996) 34

[3] U.J. Schrewe et al., in: S.M. Qaim (ed.): Nuclear Data for Science and Technology, Springer Verlag, Berlin (1992) 669

[4] M. Blann, private communication to R. Michel (1994)

[5] F.G. Perey, ORNL/TM-6062, ENDF-254, NEA Data Bank, Paris (1977)

2. Cross Sections for the Production of Residual Nuclides in Proton-Induced Reactions in Heavy Elements

M. Gloris[1], R. Michel[1], U. Herpers[2], F. Sudbrock[2], B. Holmqvist[3], H. Condé[4], P. Malmborg[5]

Recent investigations deal with the transmutation of radioactive waste to reduce the risk potential of long-lived radionuclides. This transmutation shall be achieved by neutrons produced in spallation reactions induced by protons of about 1 to 1.5 GeV energy in heavy target elements like lead or bismuth. Since primary and secondary particles produce residual nuclides in the target itself it is necessary to know their production cross sections for an estimation of the target activation. Since model calculations are not yet reliable enough [1] experimental determination of these data is still inevitable.

[1]Zentrum für Strahlenschutz und Radioökologie, Universität Hannover, F.R.G.
[2]Abteilung Nuklearchemie, Universität zu Köln, F.R.G
[3]Department of Neutron Research at Studsvik, University of Uppsala, Sweden
[4]Department of Neutron Research, University of Uppsala, Sweden
[5]The Svedberg Laboratory, University of Uppsala, Sweden

In continuation of our cross section measurements [2] we completed our irradiation experiments at the Laboratoire National Saturne/Saclay (France) in the last year. In summary it was possible to determine cross sections at ten different proton energies above 200 MeV up to 2.6 GeV. In spring 1997 we also completed our series of irradiations at the The Svedberg Laboratory/Uppsala (Sweden) giving further data below 180 MeV down to about 65 MeV.

The experimental technique employed was a pure stacked-foil-technique at TSL while we applied modified stacked-foil-techniques at LNS in order to minimize secondary particles effects. Besides target elements relevant for transmutation techniques about 30 other targets were included from carbon up to terbium. Cross sections were determined by means of off-line γ-spectrometry and accelerator mass spectrometry. Details of the experimental procedure can be found elsewhere [3].

The evaluation of data for nuclides measured by γ-spectrometry from reactions on lead resulted up to now in a dataset of over 1700 cross sections for over 100 product nuclides with half-lives spanning from about 8 hours up to 367 years. A similiar set for reactions induced in Bi is nearly completed.

Fig. 2 gives a survey over the covered range of masses of product nuclides and their cross sections at two different proton energies. At 322 MeV two regions of product nuclides can be clearly distinguished. On the one hand we find fission products located approximately at half the mass of the target while we find typical spallation products in the vicinity of the target. At an energy of 1.6 GeV the regions begin to overlap indicating the increasing influence of spallation even for nuclides with masses far away from the target. Moreover, even with γ-spectrometry it is possible to detect products with very low masses whose production must be attributed to fragmentation processes.

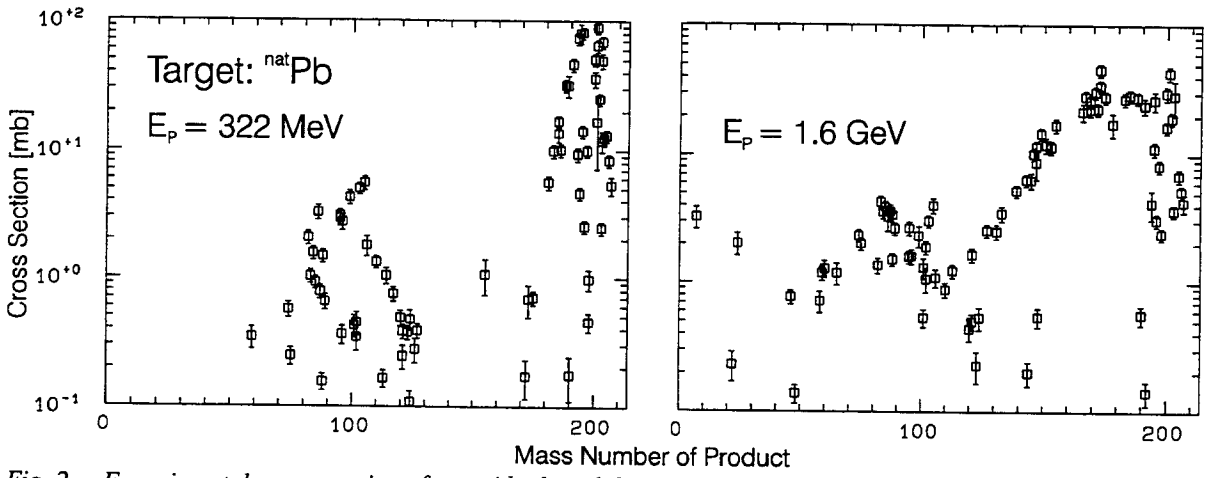

Fig. 2 Experimental cross sections for residual nuclide production by proton-induced reactions on lead as function of product mass number for two different proton energies.

Exemplary results for complete excitation functions are shown in Fig. 3 for the production of ^{127}Xe from Pb and Bi which is well suited for the demonstration of the influences of different production mechanisms. In the lower energy regime the production is governed by fission until the onset of spallation reactions, in this case at approximately 1 GeV. One more fact which can be seen is the enhanced fission cross section for ^{127}Xe from Bi with respect to Pb. This can be understood in the framework of a general increasing fission probability with the fissioning parameter Z^2/A. The differences in the production cross section fade out with increasing proton energy due to spallation reactions for which the difference in the target masses of Pb and Bi is not important.

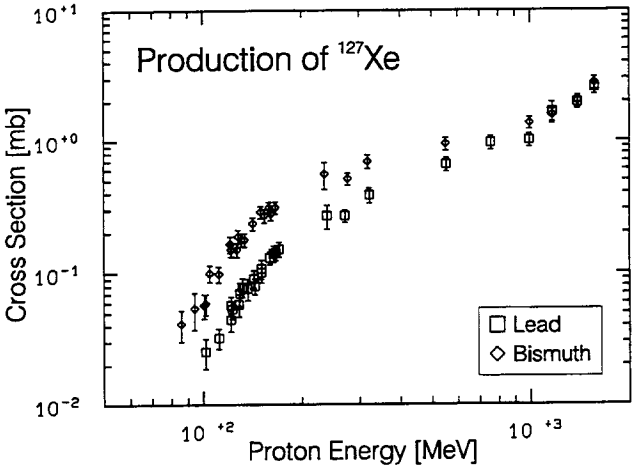

Fig. 3 Experimental excitation functions for the proton-induced production of ^{127}Xe in lead and bismuth.

Further irradiations are scheduled to be done at the Paul Scherrer Institute/Villigen (Switzerland), the first being in August 1997. These experiments will complete our knowledge of excitation functions down to threshold energies of measured product nuclides.

Acknowledgement The authors thank the authorities of LNS and TSL for the beam-time and the accelerator staffs for their essential cooperation and support. This work was supported partially by the Deutsche Forschungsgemeinschaft, Bonn, and by the CEC in the Human Capital and Mobility Programme.

References:

[1] R. Michel, P. Nagel (1997), International Codes and Model Intercomparison for Intermediate Energy Activation Yields, NEA/OECD, Paris, NSC/DOC(97)-1.

[2] R. Michel, R. Bodemann, H. Busemann, R. Daunke, M. Gloris, H.-J. Lange, B. Klug, A. Krins, I. Leya, M. Lüpke, S. Neumann, H. Reinhardt, M. Schnatz-Büttgen, U. Herpers, T. Schiekel, F. Sudbrock, B. Holmqvist, H. Condé, P. Malmborg, M. Suter, B. Dittrich-Hannen, P.-W. Kubik, H.-A. Synal, D. Filges, Cross Sections for the Production of Residual Nuclides by Low- and Medium-Energy Protons from the Target Elements C, N, O, Mg, Al, Si, Ca, Ti, V, Mn, Fe, Co, Ni, Cu, Sr, Y, Zr, Nb, Ba and Au, Nucl. Instr. Meth. Phys. Res. B129 (1997), in press.

[3] M. Gloris, R. Michel, U. Herpers, F. Sudbrock, B. Holmqvist, H. Condé, P. Malmborg, P.W. Kubik, H.-A. Synal, M. Suter, D. Filges, Proton-Induced Nuclide Production in Heavy Target Elements at Medium Energies, Proceedings 'Second International Conference on Accelerator-Driven Transmutation Technologies and Applications', Kalmar, Sweden (1996) 549.

3. Determination of Cross-Sections for the Production of Long-Lived Residual Nuclides ^{10}Be and ^{36}Cl via AMS

F. Sudbrock[1], A. Berkle[1], U. Herpers[1], R. Michel[2], M.Gloris[2], B. Holmqvist[3], H. Condé[4], P. Malmborg[5], P. W. Kubik[6], H.-A. Synal[6], M.Suter[7]

Long-lived residual nuclides dealt with here provide the tools to describe and understand the interaction of cosmic ray particles with extraterrestrial matter. In continuation of our systematic studies [cf. 1 for an overview] on the production of these long-lived radionuclides cross sections for further reactions for the production of ^{10}Be and ^{36}Cl were determined, especially for target elements with higher atomic numbers (>29). For describing the production of long-lived activation products relevant for the accelerator based waste transmutation these data have to be considered as crucial with respect to long term activation but they are by far too deficient at present. Several irradiation experiments have therefore been carried out at different locations and with different initial proton energies ranging from 100 MeV up to 2.6 GeV. For irradiations with initial energies below 200 MeV, which were accomplished at the TSL/Uppsala (S), the stacked-foil technique was applied. For irradiations with higher energies, carried out at the LNS/Saclay (F), a modified technique had to be used implying „mini-stacks" in order to diminish the influence of secondary particle fields. This design only allowed to study single energy points for a given target element.

The proton energies were calculated via the Bethe-Bloch equation in a modified form according to the work of Andersen and Ziegler [2]. For the flux monitoring the well established monitor reaction ^{27}Al(p,x)^{22}Na provided by Tobailem and de Lassus [3] was taken for energies beyond 200 MeV, whereas for lower energies this was done with the recently measured data for this excitation function measured by Steyn et al. [4].

The measurement of long-lived radionuclides by means of accelerator mass spectrometry (AMS) was performed after radiochemical separations [see 5-7 for details] at the ETH/PSI AMS facility in Zürich (CH). Details concering the AMS technique may be found elsewhere [8].

The results for the production of ^{10}Be and ^{36}Cl shown in Table 1 on the one hand close some gaps in terms of target / product combinations or energy points and on the other hand they extend the data base to heavy target elements.

Earlier measurements for the reaction Cu(p,x)^{10}Be [9] at 12 GeV give an excellent agreement suggesting that a constant value beginning with ca. 2 GeV is attained. The constant increase of the ^{10}Be production for higher target-masses proposed by Shibata et al. [9] for 12 GeV seems to hold even for energies in the region between 1 GeV and 3 GeV which this report deals with. If we -tentatively- assume the production of ^{10}Be from Pb to be constant from 2.6 GeV onwards (as seen for copper and theoretically explained by possible saturation effects for fragmentation reactions), the amazingly high cross-sections for lead found in this work [10] fit in with the description given by Shibata et al. [9].

[1] Abteilung Nuklearchemie, Universität zu Köln, F.R.G.
[2] Zentrum für Strahlenschutz und Radioökologie, Universität Hannover, F.R.G.
[3] Department of Neutron Research at Studsvik, University of Uppsala, Sweden
[4] Department of Neutron Research, University of Uppsala, Sweden
[5] The Svedberg Laboratory, University of Uppsala, Sweden
[6] Paul Scherrer Institut c/o Institut für Teilchenphysik, ETH Hönggerberg, Zürich, Switzerland
[7] Institut für Teilchenphysik, ETH Hönggerberg, Zürich, Switzerland

In addition, theoretical calculations were carried out based on two different models. The first is the hybrid model in the form of the code ALICE [11] and its recently updated version AREL. Especially for higher energies (>200MeV) calculations based on the high energy transport code (HETC [12]) were performed. A comparison of theory and experiment may indicate which reaction mechanism is more valid. The production of ^{10}Be from copper is underestimated by a factor of ten and in contrast the production of ^{36}Cl from the same target element is reproduced reasonably well. The discrepancy for ^{10}Be is interpreted in terms of fragmentation being the predominant way for the production of ^{10}Be from copper in contrast to the residual nuclide ^{36}Cl which is -for this case- merely a spallation product.

Acknowledgement:
The indispensable contributions we received from the staff of The Svedberg Laboratory/ University of Uppsala (S) and the Laboratoire National Saturne/Saclay (F) are kindly acknowledged hereby. This work was supported by the Deutsche Forschungsgemeinschaft, Bonn, by the Swedish National Research Council, Stockholm, and by the Swiss National Science Foundation, Bern

Experimental cross-sections for the proton-induced production of ^{10}Be and ^{36}Cl

	E /MeV	*ΔE /MeV*	*σ /mbarn*	*Δσ /mbarn*
^{19}F (p,x) ^{10}Be				
	170	1	0.505	0.44
	942	1	4.41	0.19
	1340	1	3.80	0.36
	2600	1	1.53	0.34
V(p,x)^{10}Be				
	92	1	0.05	0.01
	800	1	1.41	0.06
	1200	1	2.59	0.10
	2600	1	4.55	0.22
Cu(p,x)^{10}Be				
	141	1	0.001	0.0006
	158	1	0.052	0.005
	226	2	0.095	0.008
	271	1	0.132	0.011
	338	1	0.206	0.014
	374	1	0.260	0.018
	800	1	0.950	0.044
	1200	1	2.252	0.130
	1362	1	2,453	0.136
	1590	1	2.926	0.166
	2600	1	5.026	0.231
^{89}Y(p,x)^{10}Be				
	223	2	0.45	0.03
	268	1	0.41	0.03
	336	2	0.30	0.02
	372	1	0.19	0.01
Pb(p,x)^{36}Cl				
	1170	1	0.66	0.07
	1570	1	1.14	0.16
^{209}Bi(p,x)^{36}Cl				
	1170	1	1.02	0.07
	1570	1	0.72	0.05

[1] R. Michel et al. Nucl. Instr. Meth. in Phys. Res. **B103** (1995) p.183.
[2] H.H. Anderson and J.F Ziegler, Hydrogen stopping powers in all elements, Pergamon Press (1977).
[3] J-.F Tobailem and C.H. de Lassus St. Genies, CEA-N-1466 5 (1981).
[4] G.F. Steyn et al., Appl. Radiat. Isot. **41** (1990) p.315.
[5] B. Dittrich, Ph.D. thesis, University of Cologne (1990).
[6] R. Rösel, Ph.D thesis, University of Cologne (1995).
[7] T. Schiekel, Ph.D thesis, University of Cologne (1995).
[8] H.-A. Synal et al., Nucl. Instr. Meth. in Phys. Res. **B56** (1991) p. 864.
[9] S. Shibata et al., Phys. Rev **C48** (1993) p.2617.
[10] F. Sudbrock et al., in preparation (1997).
[11] M. Blann, Phys. Rev. Lett **27** (1971) p.337, errata: ibidem p. 1550.
[12] P. Cloth et al., Report Juel-2003 (1988).

INSTITUT FÜR KERNCHEMIE
UNIVERSITÄT MAINZ

1. Proton Odd-Even Effects in the Fission of the Odd-Z Compound Nucleus ^{239}Np (Z=93)

M. Davi[1], H. O. Denschlag[1], I. Tsekhanovitch[2], H. R. Faust[3], S. Oberstedt[3], M. Wöstheinrich[4]

Some time ago, a first observation of an odd-even effect of protons for the odd-Z compound nucleus ^{243}Am (Z=95) was reported by our group [1]. Odd-even effect, in this case, signifies the preferential formation of fission products with even atomic numbers among very light fission fragments.

In the fission of ^{243}Am the observation of the odd-even effect is somewhat disturbed by another effect of the closed neutron shell at N=50 taking place in the same mass range. In consequence, we attempt to confirm the proton odd-even effect in the other odd-Z compound system that is experimentally accessible to us: ^{239}Np. In this case, because of the shift of mass yield curve due to the smaller mass of the compound nucleus a disturbance by the shell closure at N=50 in the mass range of interest is not to be expected.

The measurements were performed at the recoil mass separator Lohengrin of the Institut Laue-Langevin in Grenoble (France) using targets of ^{237}Np that were converted to ^{238}Np in the target position of the mass separator. The isotope ^{238}Np is undergoing thermal neutron induced fission in the same location. The identification of the atomic numbers of the fission products took place on line after mass separation in an ionization chamber with a split anode (BIC) [2].

Some preliminary data are shown in Fig. 1. The figure shows the mass yields and the yields of the single isotopes

1. Institut für Kernchemie, Universität Mainz
2. Institute of Power Engineering Problems, Minsk, Belarus
3. Institut Laue-Langevin, Grenoble, Frankreich
4. Institut für Physik, Universität Tübingen

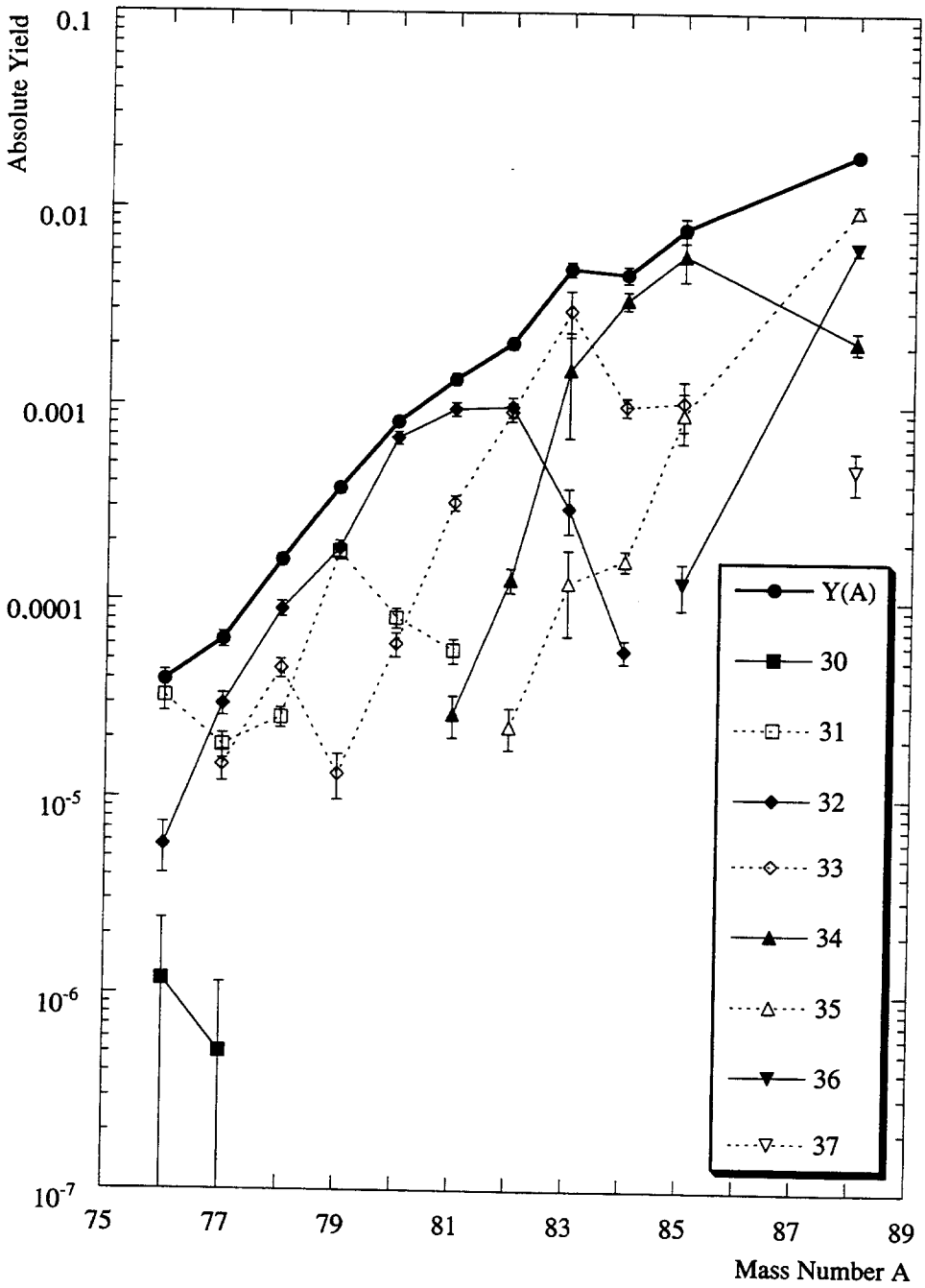

Fig. 1: Fission yield distribution in the reaction $^{238}Np(n_{th},f)$. Chain yields (uppermost curve) are shown at various mass numbers (A) and nuclide yields are plotted for the elements identified by their atomic numbers in the insert. Fragment yields for elements with even Z are shown as full symbols connected by drawn out lines and fragments with odd Z are shown by open points and dashed lines.

(identified by their atomic number Z) for various mass numbers (A=76 to 88). Data points for elements with even Z are indicated by full points and the yields are connected by drawn-out lines, whereas elements of odd Z are indicated by blank points and dashed lines. The data analysis is not finished yet; a visual inspection of the figure seems to indicate, however, already now a dominance of the even nuclei with Z=32 in the mass range from 81 to 77. This would confirm the expected odd even effect in the very asymmetric fission of the odd-Z compound nucleus ^{239}Np.

Acknowledgement: This work was supported by the Bundesministerium für Forschung und Technologie under contract No. 06-MZ-465 and 06-MZ-476.

References

1. P. Stumpf, H. O. Denschlag, H. R. Faust: Odd-Even and Shell Effects in the Fission of the Odd Compound Nucleus ^{243}Am (Z=95), in S. M. Qaim (Ed.) Progress Report on Nuclear Data Research in the Federal Republic of Germany, Report NEA/NSC/DOC(95)10, INDC(Ger)-040 Jül-3086
2. P. Stumpf, U. Güttler, H. O. Denschlag, H. R. Faust: Odd-Even Effects in the Reaction ^{241}Am(2n,f), in (S.M. Qaim, Ed.) Nuclear Data for Science and Technology, Springer Verlag, Berlin (1992), p. 145
3. J. P. Bocquet, R. Brissot, H. R. Faust; Nucl. Instr. Methods in Phys. Res. A267, 466-472 (1988)

INSTITUT FÜR KERNCHEMIE
PHILIPPS-UNIVERSITÄT MARBURG

Determination of the Half-Life of ^{105m}Rh

A. Kronenberg, K. Siemon, R. Weber, R.A. Esterlund and P. Patzelt

For well over two score years, the half-life of ^{105m}Rh has been uncertain [1] by nearly a factor of two. The earliest value in the literature (1951), from R.B. Duffield and L.M. Langer [2], is given as 45 s, without any error. In strong contrast, a subsequent measurement [3] in 1955 by J.W. Winchester and C.D. Coryell yielded a highly divergent value of about 30 s. As a result, the editors of Nuclear Data Sheets have stated [1]: "As no uncertainty is given by (Duffield and Langer) and a large discrepancy exists with the value of (Winchester and Coryell), the evaluators strongly recommend that the $T_{1/2}$ of this level be remeasured". Until now, this problem has never been addressed. The resolution of this inconsistency is our goal here.

A simplified decay scheme for the nuclides of interest in the A = 105 mass chain is depicted in Fig. 1. It is readily apparent that the short-lived ^{105m}Rh daughter can be chemically extracted at regular intervals for $T_{1/2}$ measurements from the relatively long-lived ^{105}Ru mother. The ^{105}Ru mother in turn can be produced in a number of ways, *e.g.*, *via* thermal-neutron irradiation of either ^{235}U, whereby ^{105}Ru is produced as a fission product, or $RuCl_3$, whereby ^{105}Ru is formed directly *via* radiative capture. We have chosen the former method, utilizing the TRIGA reactor at the Institut für Kernchemie Mainz. Exactly 2.0 mg of ^{235}U (isotopic purity > 93%) in the form of $UO_2(NO_3)_2 \cdot 6H_2O$ powder in a quartz ampoule was irradiated for 6 h with a neutron flux of 7×10^{11} n/cm^2/s. The procedure for the fast chemical separation of Rh from other fission products was suggested by N. Trautmann [4], based on a separation procedure for Ru by Skarnemark, *et al.* [5]. Very briefly, Ru was first oxidized to RuO_4 with Ce^{IV}, and then extracted from an acidic aqueous solution containing other fission products using CCl_4. After waiting 7-8 minutes for radioactive equilibrium between ^{105}Ru and ^{105m}Rh to be attained, the ^{105m}Rh was then back-extracted from the CCl_4 phase into the aqueous Ce^{IV} phase and placed in a plastic test tube for radioactive assay. To improve counting statistics, this procedure of back-extraction followed by measurement was repeated several times. Details are given elsewhere [6].

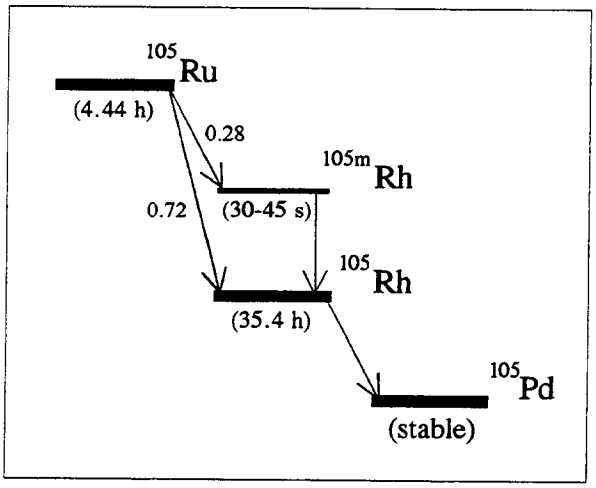

Fig. 1: Simplified decay scheme for ^{105}Ru.

As may be seen from Fig. 1, ^{105m}Rh decays *via* internal transition ($E\gamma$ = 129.78 keV), and hence may easily be assayed *via* gamma-ray spectrometry. For each sample, gamma spec-

tra were taken continuously for equal counting periods of 12 s, over a total measuring interval of about 1500 s, using either a calibrated well-type NaI crystal or Ge(Li) detector connected to a pulse-height analyzer operated in the 4096-channel mode, along with the usual associated electronics. Although the Ge(Li) detector achieves much higher energy resolution, the NaI detector offers the advantage of much higher efficiency (and thereby better counting statistics). In the latter case, data were also collected from a single-channel analyzer (SCA) centered on the 129.78-keV peak, thus yielding decay data from three sources. The sum of three of the early Ge(Li) spectra is shown in Fig. 2. Aside from the dominant 129.78-keV peak of ^{105m}Rh, there are only very small peaks from either ^{105}Ru (activity < 3%) or ^{105g}Rh.

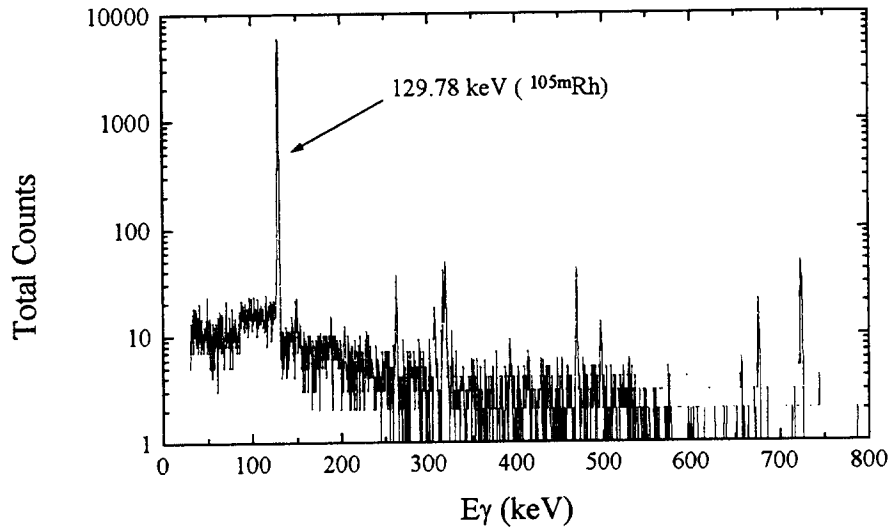

Fig. 2: Summed Ge(Li) gamma-spectra for the Rh chemical fraction.

The gamma spectra were assayed using either the computer program GAMMAW [7] for the Ge(Li) data or the computer program SODIGAM [8] for the NaI data. The count rates for the 129.78-keV gamma-ray peak as a function of time were corrected for dead-time, and decay curves were constructed which were subjected to analysis using the program CLSQ [9]. The best decay curve resulted from the NaI SCA data, and it is shown in Fig. 3(a). It consists of two components, a short-lived one (^{105m}Rh), and a minor long-lived one (^{105}Ru). When the 4.44-h ^{105}Ru component is subtracted, we obtain the single-component decay curve shown in Fig. 3(b) for ^{105m}Rh. The results of the decay-curve analysis in this case yielded a $T_{1/2}$ for ^{105m}Rh of 42.89 ± 0.12 sec, with a reduced chi-square (χ^2/ν) of 0.86, indicating the validity of the analysis and the corresponding error. The error on this $T_{1/2}$ was verified, using the algorithms described in [10]. All the other $T_{1/2}$ values are consistent with this value. As the errors on the other values are significantly larger, the new weighted mean value for the $T_{1/2}$ of ^{105m}Rh is not appreciably different from the best decay-curve value, *i.e.*,

$$\mathbf{T_{1/2}\,(^{105m}Rh) = 42.9 \pm 0.1\ s}$$

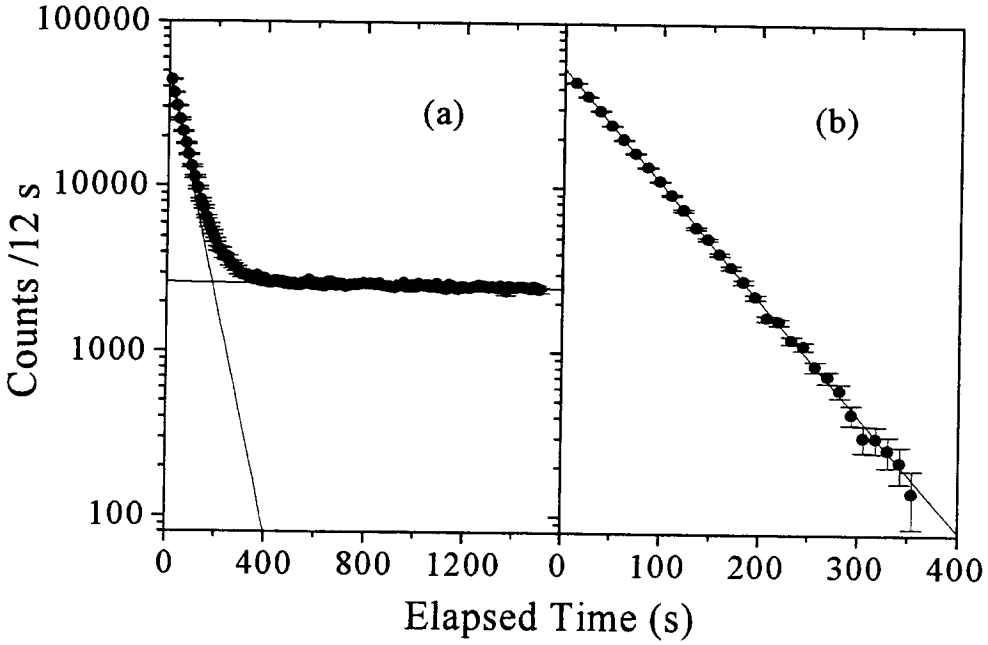

Fig. 3: Decay-curve data for the Rh chemical fraction (see text).

References

[1] D. De Frenne, E. Jacobs, M. Verboven and P. De Gelder: Nuclear Data Sheets for A = 105, Nucl. Data Sheets **47**, 261 (1986).

[2] R.B. Duffield and L.M. Langer: Radioactivities of ^{105}Ru, ^{105}Rh, ^{84}Br, and ^{83}Br, Phys. Rev. **81**, 203 (1951).

[3] J.W. Winchester and C.D. Coryell: Fission Yields in the Valley Region, MIT-LNS Annual Progr. Rept. **AECU-3110**, 29 (1955), as well as J.W. Winchester: *A Study of Fission Products in the Region of Mass Numbers 103 to 131.* PhD thesis 1955 (Massachusetts Institute of Technology, Cambridge, Massachusetts).

[4] N. Trautmann, private communication (1997).

[5] G. Skarnemark, K. Broden, M. Yun, N. Kaffrell and N. Trautmann: Rapid Continuous Separation Procedures for Arsenic and Ruthenium from Complex Reaction Product Mixtures, Radiochimica Acta **33**, 97 (1983).

[6] A. Kronenberg, Diplomarbeit, Institut für Kernchemie Marburg (in preparation).

[7] W. Westmeier: Spektrenanalyseprogramm GAMMAW, Version 17.01 (June 1996), Gesellschaft für Kernspektrometrie mbH, D-35085 Ebsdorfergrund-Mölln, Germany.

[8] W. Westmeier: Spektrenanalyseprogramm SODIGAM, Version 7.04 (June 1987), Gesellschaft für Kernspektrometrie mbH, D-35085 Ebsdorfergrund-Mölln, Germany.

[9] J.B. Cumming: CLSQ, The Brookhaven Decay-Curve Analysis Program, in *Application of Computers to Nuclear- and Radiochemistry*, ed. G.D. O'Kelly (National Academy of Sciences, National Series rept. NAS NS-3107, Washington, 1962) p.25.

[10] G. Azuelos, J.E. Crawford and J.E. Kitching: Precision Half-Life Measurement using Ge(Li) Detectors, Nucl. Instr. Meth. **117**, 233 (1974) as well as J.A. Becker, R.A. Chalmers, B.A. Watson and D.H. Wilkinson: Precision Measurement of Nuclide Half-Lives, Nucl. Instr. Meth. **155**, 211 (1978).

FRM-REAKTORSTATION GARCHING
FACHBEREICH PHYSIK
TECHNISCHE UNIVERSITÄT MÜNCHEN

Interaction of Slow Neutrons with Cobalt and Tin*

K. Knopf, W. Waschkowski, A. Aleksejevs[a)], S. Barkanova[a)], and J. Tambergs[a)]

Coherent neutron scattering lengths and total cross sections have been measured on samples of Co, Sn and on isotopically enriched Sn-oxides. The following data were obtained:

- the coherent scattering lengths (in fm) of the bound atoms ^{59}Co (2.49 ± 0.02), ^{nat}Sn (6.22 ± 0.01), ^{116}Sn (6.10 ± 0.01), ^{117}Sn (6.59 ± 0.08), ^{118}Sn (6.23 ± 0.04), ^{119}Sn (6.28 ± 0.03), ^{120}Sn (6.67 ± 0.04), ^{122}Sn (5.93 ± 0.03), and ^{124}Sn (6.15 ± 0.03);
- the thermal absorption cross sections (in b) ^{nat}Sn (0.569 ± 0.005), ^{116}Sn (0.50 ± 0.03), ^{117}Sn (0.77 ± 0.06), ^{118}Sn (0.24 ± 0.06), ^{119}Sn (2.19 ± 0.06), ^{120}Sn (0.55 ± 0.06), ^{122}Sn (0.19 ± 0.06), and ^{124}Sn (0.43 ± 0.06).

New bound levels were evaluated for the investigated nuclei. In combination with the resonance parameters the measured scattering lengths allowed the determination of potential scattering radii R' which are of particular interest for the check of the optical model.

---

*Z. Naturforsch. **52 a**, 270 - 278

a) Nuclear Research Center, 31 Miera Str., LV-2169 Salaspils-1, Latvia

PHYSIKALISCH-TECHNISCHE BUNDESANSTALT BRAUNSCHWEIG

1. Measurement of the $^{52}Cr(n,p)^{52}V$ Cross Section between 7.9 and 14.4 MeV

W. Mannhart, D. Schmidt, D.L. Smith*

At 15 neutron energies between 7.89 and 14.45 MeV, cross section data of the $^{52}Cr(n,p)^{52}V$ reaction were measured. Neutrons were produced via the $D(d,n)^3He$ reaction with a deuterium gas target. Extensive corrections for background and deuterium breakup neutrons were applied. The data are based on the $^{238}U(n,f)$ cross sections taken from the ENDF/B-VI evaluation. The typical uncertainties of our data are between 3 and 4%. The neutron energy scale is based on TOF measurements and the mean neutron energy is defined within ± 20 keV. The experimental procedure is similar to previous measurements [1].

Our data were corrected for a weak $^{53}Cr(n,np)^{52}V$ contribution and are shown in Fig. 1 in comparison with other experiments given in the EXFOR database [2], and with the ENDF/B-VI, the EFF-2.4 and the IRK-94 [3] evaluations. Over the whole energy range, none of the evaluations is fully consistent with our data. Below 12 MeV, the EFF-2.4 evaluation shows a fair agreement with our data and above 12 MeV, our data tend to support the ENDF/B-VI evaluation. The IRK-94 evaluation, strongly based on available experiments is, above 13 MeV, mainly guided by the experiments of Ikeda (1988) and Kawade (1990). It cannot be excluded that the two experiments used identical samples. The data of Ikeda (1988) are lower than ours and those of ENDF/B-VI by about 10%. A deviation of the same

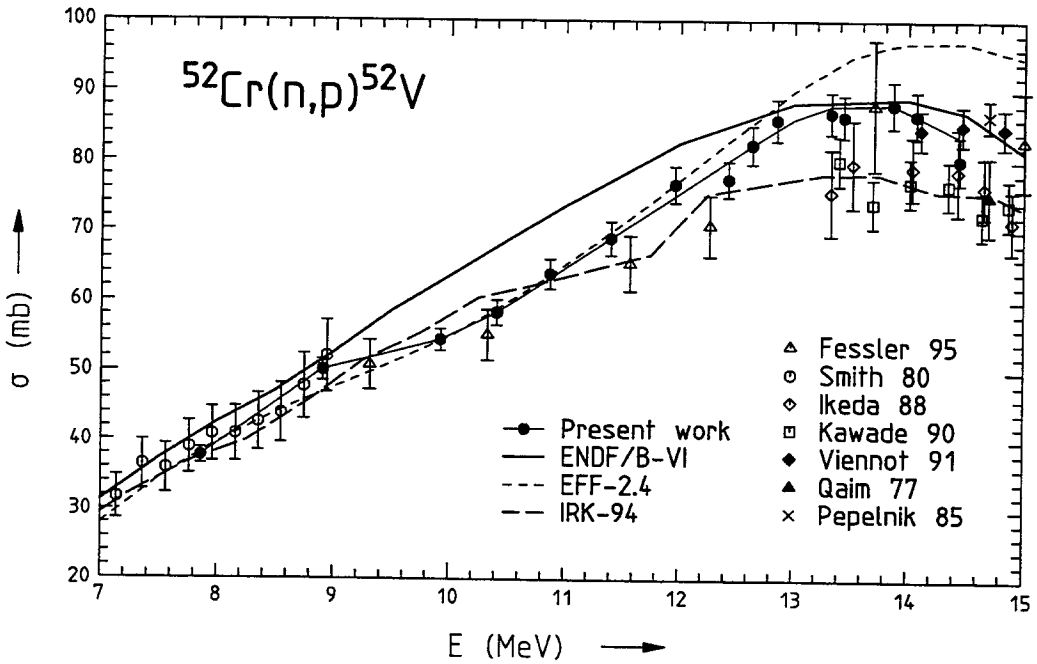

Fig. 1 Cross section of the $^{52}Cr(n,p)^{52}V$ reaction

*Argonne National Laboratory, Argonne, USA

magnitude can also be observed in the database of the $^{52}Cr(n,2n)^{51}Cr$ reaction (see next contribution) between the data of Ikeda (1988) and those of other experiments including our recent measurements. This coincidence suggests difficulties with the sample mass in the experiment of Ikeda (1988). The IRK-94 evaluation is also supported by the experiment [4] of Fessler (1995). This experiment consists of two different parts. Up to 12.3 MeV, the data are based on a D-D neutron source and above 13.75 MeV, a D-T neutron source was used. The high-energy data agree very well with our data, with the data of Viennot (1991) and with ENDF/B-VI. Below 12.3 MeV, the deviation between the data of Fessler (1995) and our data, both measured with a D-D neutron source, cannot be explained by an inconsistent breakup correction, which is < 1% at 12.3 MeV. However, a shift of the energy scale of about -500 keV in the experiment of Fessler (1995) would resolve the differences.

2. Measurement of the $^{52}Cr(n,2n)^{51}Cr$ Cross Section between Threshold and 14.4 MeV

W. Mannhart, D. Schmidt, D.L. Smith*

Using the experimental technique described in the previous contribution, cross section data of the $^{52}Cr(n,2n)^{51}Cr$ reaction were measured at 8 neutron energies between the reaction threshold and 14.45 MeV. High-purity metallic samples, 10 mm in diameter and 1 mm thick, were used in the experiment. Due to the mechanical brittleness of chromium, the samples were fabricated by a special laser cutting technique.

Below the reaction threshold of 12.271 MeV, additional measurements were performed to identify a possible contribution to the measured data from the $^{50}Cr(n,\gamma)^{51}Cr$ reaction channel. Within the measurement limits, traces of such a contamination were not detected. With the exception of the data point at the lowest neutron energy measured, the uncertainties of our data were between 5.5% and 3.7%, decreasing with increasing neutron energy.

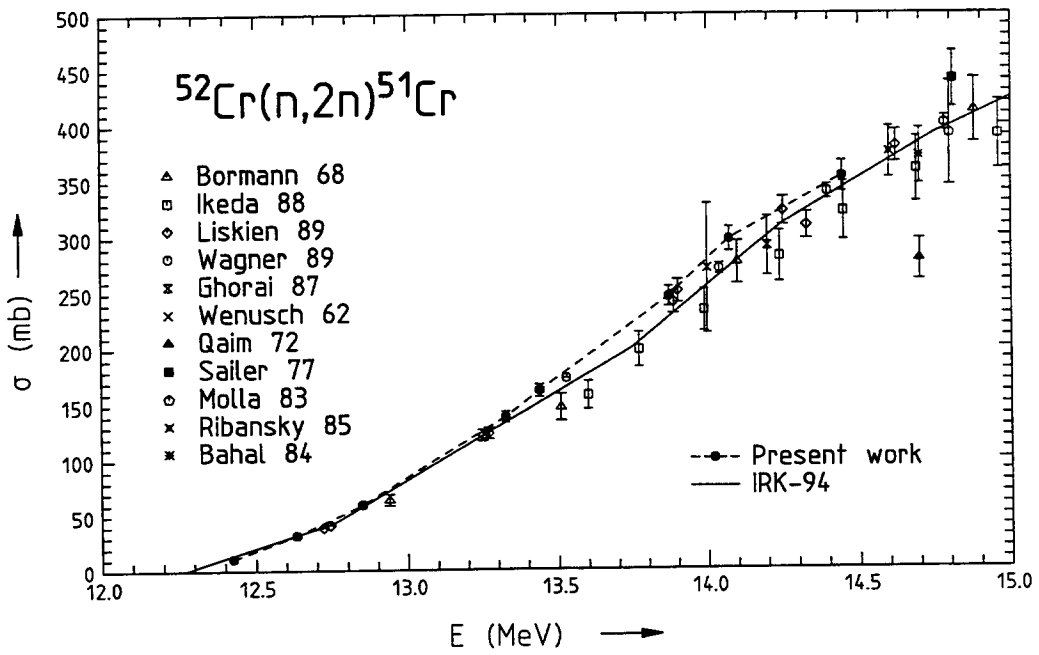

Fig. 2 Cross section of the $^{52}Cr(n,2n)^{51}Cr$ reaction

Our experimental data are given in Fig. 2 and compared with other experiments and with the IRK-94 evaluation [3]. Above 12.8 MeV, our data consistently exceed the IRK-94 evaluation, between 2% at 12.8 MeV and 9% at 14.1 MeV. Our data are in excellent agreement with the experiment [5] of Liskien (1989) and contradict, especially around 14 MeV, the data [6] of Wagner (1989). The data set [7] of Ikeda (1988) clearly underestimates the cross section of this reaction.

3. Neutron Scattering on ^{51}V at Energies between 8 MeV and 15 MeV
D. Schmidt, W. Mannhart, Zhou Chenwei**

After iron, lead and chromium, vanadium was used to continue the neutron scattering cross section measurements on fusion-relevant materials. There is a lack of data in the energy range between 11 MeV and 14 MeV. Below 10 MeV, a comprehensive data set was measured at ANL [8].

Measurements were carried out with a sample of natural vanadium (^{51}V content: 99.75%) at 11 incident energies between 7.99 MeV and 14.37 MeV. The measurement arrangement, data reduction and correction procedures were the same as described for the iron measurement [9].

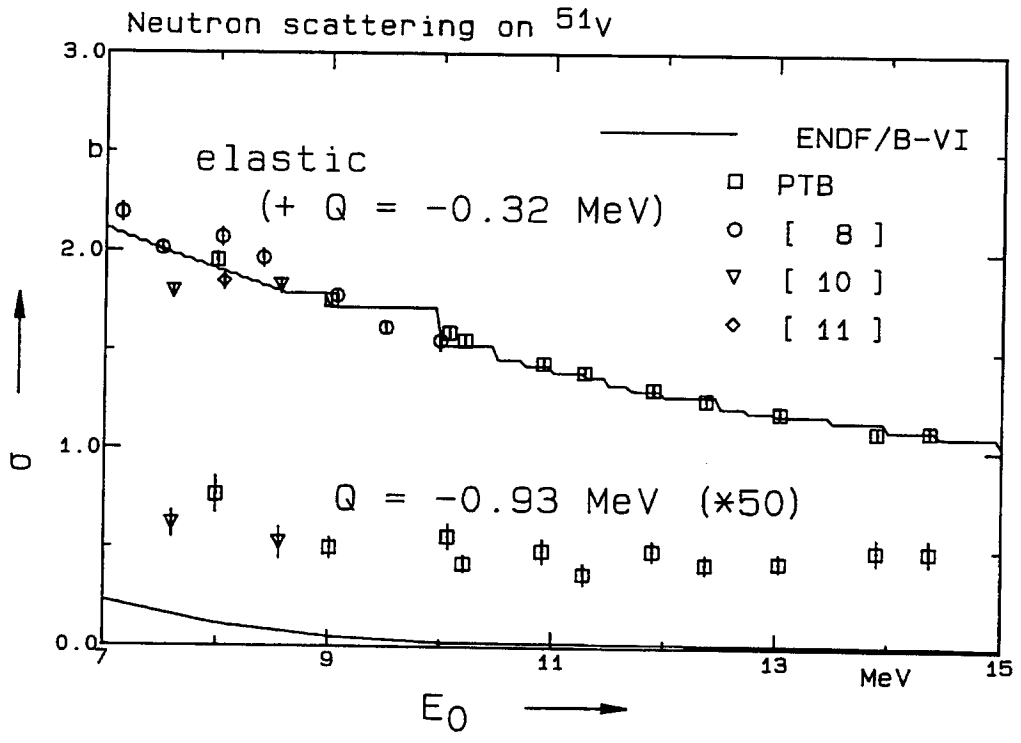

Fig. 3 Angle-integrated elastic and inelastic cross sections from ^{51}V (note the scale expansion factor of 50); data from the literature [8,10,11] and from the ENDF/B-VI evaluation are included.

**Permanent address: CIAE Beijing, P.R. China

Because the first level of ^{51}V has an excitation energy of $E_{ex} = 0.32$ MeV, only the cross section sum of the elastic and this inelastic scattering fraction could be determined. Inelastic cross sections were determined for the second level ($E_{ex} = 0.92$ MeV) and for the sum of the third and fourth excited states ($E_{ex} = 1.61 / 1.81$ MeV).

Fig. 3 shows some results, together with other measurements and with the ENDF/B-VI evaluation. The agreement is satisfactory. The evaluation of the inelastic data is too small, because no proper reaction model is available.

4. Double-differential Neutron Emission Cross Sections from Natural Lead in the Energy Region between 8 MeV and 15 MeV

D. Schmidt, W. Mannhart, B.R.L. Siebert

The measurement technique and data processing used until now to determine partial differential cross sections were extended to obtain double-differential emission cross sections (DDX). Because the DD reaction is used, disturbing breakup neutrons are superimposed on the inelastically scattered DD neutrons. The fraction of scattered breakup neutrons was calculated with a realistic Monte Carlo simulation and then subtracted.

The data for the breakup simulation were taken from the ENDF/B-VI evaluation. These data, in particular the differential elastic ones, are not sufficiently exact; they have therefore to be

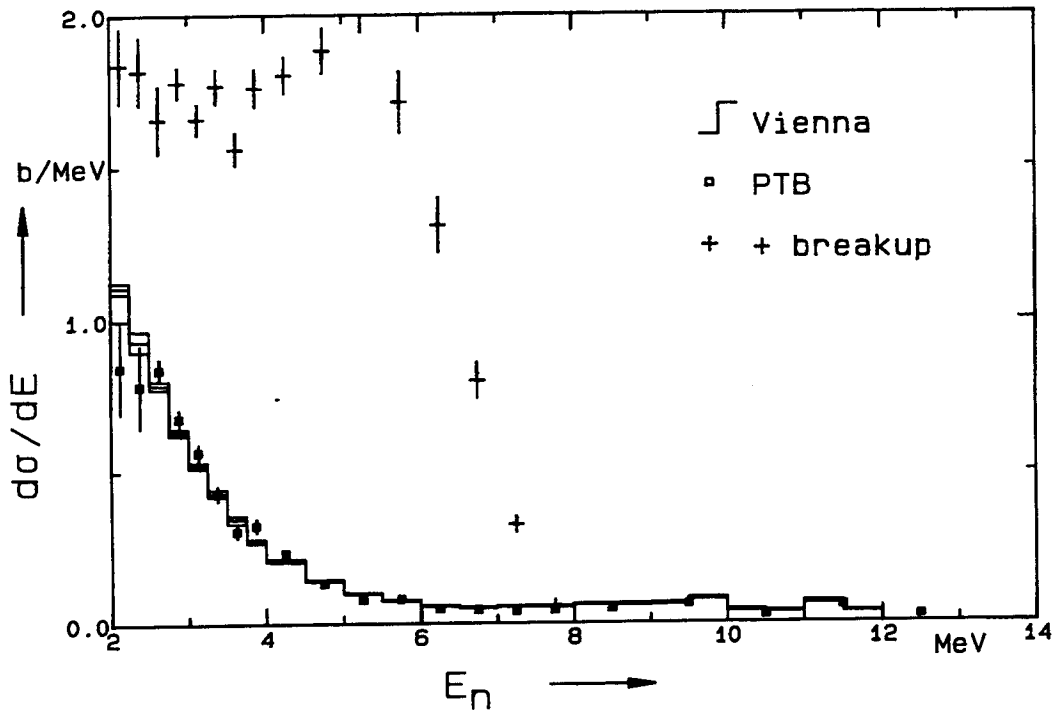

Fig. 4 Angle-integrated neutron emission spectrum of natural lead at the incident energy $E_0 = 14.23$ MeV (PTB) and at $E_0 = 14.07$ MeV (Vienna [12]); "+ breakup": pseudo-data without breakup subtraction.

adjusted. This was done using additional scattering measurements with the pure breakup reaction ^{4}He(d,n). If all data were adjusted to properly describe the scattering of the ^{4}He(d,n) neutrons, they could be used successfully to subtract the DD breakup fraction.

Fig. 4 shows the angle-integrated emission spectrum of lead at the incident energy $E_0 = 14.23$ MeV, compared with a recent measurement at the IRK Vienna [12]. The agreement is satisfactory, even the subtracted breakup fraction in some cases exceeds the DDX by a factor of 10. The result demonstrates the successful data adjustment.

Fig. 5 gives DDX in several energy intervals as a function of the angle, also compared with the IRK data. The uncertainties of our data are rather high due to the experimental conditions as well as the breakup subtraction.

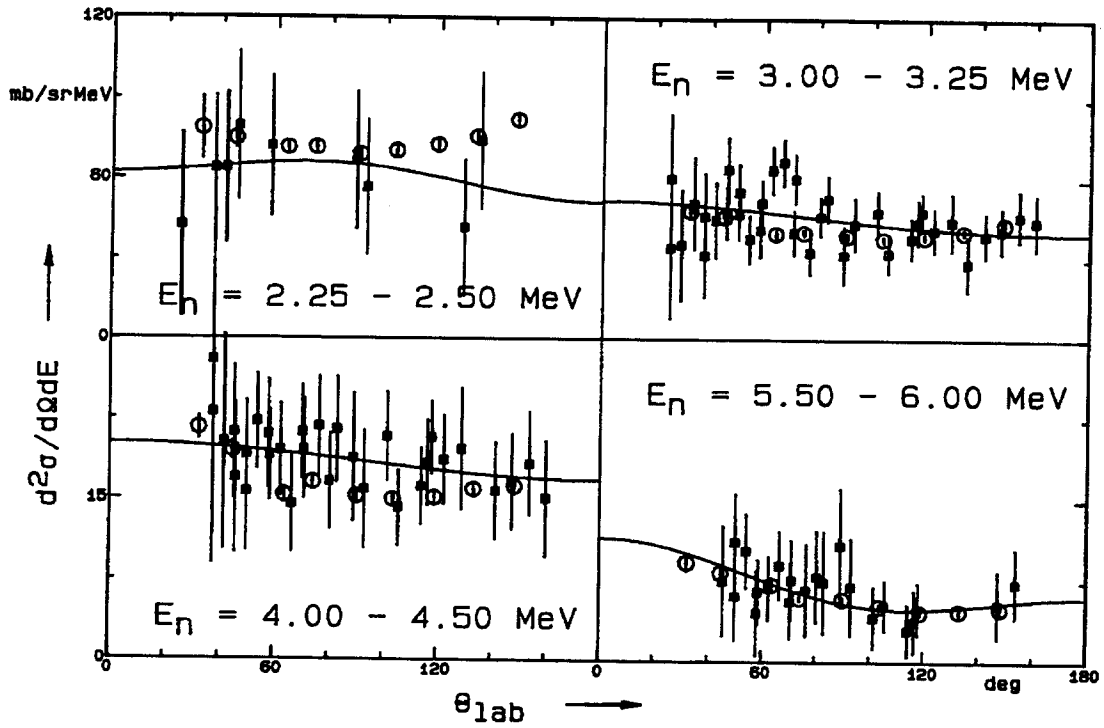

Fig. 5 DDX of natural lead as a function of the angle for emission energy intervals given at the indident energy $E_0 = 14.23$ MeV (PTB, squares) and at $E_0 = 14.07$ MeV (Vienna [12], circles).

With the data adjusted at the highest incident energy ($E_0 = 14.23$ MeV), the breakup subtraction was also made at lower incident energies, and the corresponding DDX could be obtained. Further results, details of the procedure and possibilities of improvement of this method will be published soon.

5. Half-Life Measurements on Isotopes of Europium

H. Schrader, U. Schötzig

Half-lives of Eu isotopes were measured using ionization chambers and semiconductor detectors. Regular measurements were performed over a period of more than 16 years. The long-term stability of the efficiency of the ionization chamber was carefully checked with a ^{226}Ra reference source. Results are summarized in Table 1; standard uncertainties are given in parentheses in terms of the last digit.

Table 1: Half-lives ($T_{1/2}$) of Eu nuclides

$T_{1/2}(^{152}Eu)$	=	4936.6 (20)	d
$T_{1/2}(^{154}Eu)$	=	3138.1 (16)	d
$T_{1/2}(^{155}Eu)$	=	1739 (8)	d

References

[1] W. Mannhart, D. Schmidt, Xia Haihong, Proc. Int. Conf. on Nuclear Data for Science and Technology, Gatlinburg (1994) 285

[2] EXFOR Database, NEA Data Bank, OECD, Paris

[3] V. Pronyaev, S. Tagesen, H. Vonach, S. Badikov, Physics Data 13-8 (1995)

[4] A. Fessler, KFA Jülich, private communication (1995)

[5] H. Liskien et al., Ann. Nucl. Energy 16 (1989) 563

[6] M. Wagner et al., Ann. Nucl. Energy 16 (1989) 623

[7] Y. Ikeda et al., Report JAERI-1312, JAERI, Tokai-mura (1988)

[8] A.B. Smith et al., Report ANL/NDM-106, ANL Argonne/USA (1988) and EXFOR 13135

[9] D. Schmidt et al., Report PTB-N-20, PTB Braunschweig/Germany (1994)

[10] W.E. Kinney et al., Report ORNL-4551, ORNL Oak Ridge/USA (1970) and EXFOR 10110

[11] B. Holmqvist et al., Nucl. Phys. A 188 (1972) 24 and EXFOR 20019

[12] P. Steier, IRK Vienna/Austria, private communication (1994)

APPENDIX

Addresses of Contributing Laboratories

Institut für Kernphysik III
Director: Prof. Dr. G. Schatz
Senior reporter: Dr. F. Käppeler
Forschungszentrum Karlsruhe
Postfach 36 40
76021 Karlsruhe

Institut für Materialforschung I
Director: Prof. Dr. K.-H. Zum Gahr
Senior reporter: Dr. E. Daum
Forschungszentrum Karlsruhe
Postfach 36 40
76021 Karlsruhe

Institut für Neutronenphysik
und Reaktortechnik
Director: Prof. Dr. G. Kessler
Senior reporter: Dr. U. Fischer
Forschungszentrum Karlsruhe
Postfach 36 40
76021 Karlsruhe

Institut für Nuklearchemie
Director: Prof. Dr. H.H. Coenen
Senior reporter: Prof. Dr. S.M. Qaim
Forschungszentrum Jülich
Postfach 19 13
52425 Jülich

Institut für Kernphysik
Director: Prof. Dr. O.W.B. Schult
Senior reporter: Dr. H. Ohm
Forschungszentrum Jülich
Postfach 19 13
52425 Jülich

Institut für Kern- und Teilchenphysik
Director: Prof. Dr. K.R. Schubert
Senior reporter: Prof. Dr. K. Seidel
Technische Universität Dresden
Mommsenstr. 13
01062 Dresden

Zentrum für Strahlenschutz und Radioökologie
Head and senior reporter: Prof. Dr. R. Michel
Universität Hannover
Am Kleinen Felde 30
30167 Hannover

Abteilung Nuklearchemie
Head: Prof. Dr. H.H. Coenen
Senior reporter: Dr. U. Herpers
Universität zu Köln
Otto-Fischer-Str. 12-14
50674 Köln

Institut für Kernchemie
Head and senior reporter: Prof. Dr. J.O. Denschlag
Universität Mainz
Fritz-Strassmann-Weg 2
55128 Mainz

Fachbereich Physikalische Chemie
Kernchemie
Senior reporter: Prof. Dr. P. Patzelt
Philips-Universität Marburg
Lahnberge
35043 Marburg/Lahn

FRM-Reaktorstation Garching
Fachbereich Physik
Senior reporter: Dr. W. Waschkowski
Technische Universität München
85747 Garching/München

Physikalisch-Technische Bundesanstalt
Abteilung Ionisierende Strahlung
Director: Prof. Dr. G. Dietze
Senior reporter: Dr. W. Mannhart
Bundesallee 100
38116 Braunschweig